ISTANBUL TECHNICAL UNIVERSITY ★ INSTITUTE OF SCIENCE AND TECHNOLOGY

SYNTHESIS AND CHARACTERISATION OF POLYACRYLAMIDE – LAPONITE NANOCOMPOSITE HYDROGELS

M. Sc. Thesis by
Volkan CAN

Department : **Polymer Science and Technology (PST)**

Programme: **Polymer Science and Technology (PST)**

Supervisor: Prof. Dr. Oğuz OKAY

JANUARY 2008

ISTANBUL TECHNICAL UNIVERSITY ★ INSTITUTE OF SCIENCE AND TECHNOLOGY

SYNTHESIS AND CHARACTERISATION OF POLYACRYLAMIDE – LAPONITE NANOCOMPOSITE HYDROGELS

M. Sc. Thesis by

Volkan CAN

(515041038)

Date of submission : 24 December 2007
Date of defence examination: 30 January 2008

Supervisor : Prof. Dr. Oğuz OKAY

Members of the Examining Committee

Prof.Dr. Mine YURTSEVER (ITÜ.)

Doc. Dr Gülten GÜRDAĞ (IÜ.)

JANUARY 2008

İSTANBUL TEKNİK ÜNİVERSİTESİ ★ FEN BİLİMLERİ ENSTİTÜSÜ

POLİAKRİLAMİD – LAPONİT NANOKOMPOZİT HİDROJELLERİNİN SENTEZİ VE KARAKTERİZASYONU

YÜKSEK LİSANS TEZİ

Volkan CAN

(515041038)

Tezin Enstitüye Verildiği Tarih : 24 Aralık 2007
Tezin Savunulduğu Tarih : 30 Ocak 2008

Tez Danışmanı : **Prof. Dr. Oğuz OKAY**

Diğer Jüri Üyeleri **Prof.Dr. Mine YURTSEVER (ITÜ.)**

Doc. Dr Gülten GÜRDAĞ (IÜ.)

OCAK 2008

ACKNOWLEDGEMENTS

I would like to express my gratitute to Prof. Dr. Oğuz OKAY for his guidance and continuous encouragement through this work.

I am gratreful to Dr. Nermin ORAKDÖĞEN and Dr. Suzan ABDURRAHMANOĞLU for their willingness to help and suggestions. I also want to thank to my dear collegues M. Murat ÖZMEN, Deniz CEYLAN, Saadet DOĞU, Miray ÇİLİNGİR and Maria Valentina DINU for their support.

Above all, I want to present my gratittude to my beloved family that gave me the endless support and tolerance in every little moment of my life.

January, 2008 Volkan CAN

TABLE OF CONTENTS

LIST OF FIGURES

Page Numbers

LIST OF TABLES **Page Numbers**

LIST OF SYMBOLS

n_1, n_2	:	Number of solvent and polymer molecules
n_o	:	Total number of lattice sites
x	:	Number of segments of a polymer chain
V_1	:	Molar volume of solvent
i	:	Number of chains added to the lattice
z	:	Coordination number of the lattice
Ω	:	Total number of conformations
v_1, v_2	:	Volume fractions of solvent and polymer molecule
ΔS_m	:	Entropy change of mixing
w_{ij}	:	Energy of the formation of a contact between a pair of segments of molecules i and j
ΔH_m	:	Enthalpy change of mixing
χ	:	Polymer-solvent interaction parameter
k	:	Boltzman's constant
T	:	Absolute temperature (K)
ΔG_m	:	Free energy change of mixing
p	:	Probability of a one end of the chain located within a small element
s	:	Entropy of the chain
λ	:	Deformation ratio (deformed length/initial length)
λ_1, λ_2, λ_3	:	Macroscopic deformation ratios of the network chains
r_o	:	End to end distance of an individual chain in the unstrained state
r	:	End to end distance after deformation
ΔS_{el}	:	Entropy change during deformation
$\overline{r_o^2}$	:	Mean-square end-to-end distance of the chains
ΔG_{el}	:	Free energy change during deformation
v_2^0	:	Volume fraction of the crosslinked polymer after the gel preparation
ΔG	:	Free energy change during swelling
V_o, V	:	Gel volumes after the gel preparation and after swelling
μ_1, μ_1^o	:	Chemical potentials of solvents inside and outside the gel
v_2	:	Volume fraction of crosslinked polymer in the gel
v_e	:	Number of chains per unit volume of the network
ρ	:	Polymer density

$\overline{M_c}$	:	Molecular weight of the network chains
π_i	:	Osmotic pressure due to the concentration difference
f	:	Mole fraction of ionic segments in the network chains
ΔA_{el}	:	Helmholtz free energy
W	:	Work of deformation
ν	:	Concentration of the network chains.
R	:	Gas constant
D , D_o	:	Diameter of the hydrogels after equilibrium swelling and after preparation
q_v	:	Volume swelling ratio
g	:	Gravitational acceleration
l_o , l	:	Initial undeformed and deformed lengths
A	:	Cross-sectional area of the specimen
c	:	Initial monomer concentration
G_o	:	Elastic modulus of gel after preparation
G	:	Elastic modulus of gel
$M_{c,chem}$	:	Chemical molecular weight of the network chains
X	:	Crosslinker ratio
M_r	:	Molecular weight of polymer repeated units.

SYNTHESIS AND CHARACTERISATION OF POLYACRYLAMIDE – LAPONITE NANOCOMPOSITE HYDROGELS

SUMMARY

The swelling behavior and the elastic properties of nanocomposite hydrogels have been investigated. The hydrogels were prepared by free-radical polymerization of the monomer acrylamide (AAm) in aqueous clay suspensions at 5^0C. Laponite XLS with a radius of 25 nm was used as clay particles in the hydrogel preparation. The reactions were carried out in the presence of the chemical crosslinker N, N'-methylenebis(acrylamide) (BAAm).

It was found that the nanocomposite hydrogels based on PAAm as the hydrophilic polymer component and Laponite XLS as the clay component exhibit unusual swelling behavior in water. They first rapidly swell and attain a maximum swelling ratio after about one day. Further increase in the swelling time results in the deswelling of the gels until they reach a limiting swelling ratio after about 5 days. This type of swelling behavior is observable only, when the clay concentration in the hydrogel is above a critical concentration. Swelling measurements combined with the elasticity tests show that the effective crosslink density, ν_e, of the hydrogels first decreases, but then increases with increasing time of swelling. The extent of the variations in ν_e becomes significant as the clay content is increased or, as the chemical crosslinker ratio X is decreased. The results were explained in terms of the rearrangements of the highly entangled polymer chains and clay particles during the course of swelling. It was also shown that the nanocomposite hydrogels become unstable and dissolve in dilute aqueous solutions of acetone or poly(ethylene oxide) (PEO) of molecular weight 10000 g/mol.

POLİAKRİLAMİD – LAPONİT NANOKOMPOZİT HİDROJELLERİNİN SENTEZİ VE KARAKTERİZASYONU

ÖZET

Bu çalışma kapsamında, nanokompozit hidrojellerin şişme ve elastik davranışları araştırılmıştır. Hidrojeller, sulu kil süspansiyonu içerisinde akrilamid (AAm) monomerinin serbest radikal polimerizasyonu ile 5 ^{0}C'de sentezlenmiştir. Reaksiyonlar kimyasal bir çapraz bağlayıcı olan N,N'-metilenbis(akrilamid) (BAAm) varlığında gerçekleştirilmiştir.

Bulgular, hidrofilik polimer bileşeni olan PAAm ve kil bileşeni olan Laponit XLS ile sentezlenen nanokompozit hidrojellerin normal jellerde görülmeyen bir şişme davranışına sahip olduunu göstermiştir. Buna göre jeller suya atıldıklarında, yaklaşık bir gün süreyle şişerek bir maksimum değere ulaşmaktadır. Jellerin su içerisinde kalma süreleri arttırıldığında ise şişme değerleri azalarak, yaklaşık 5 gün içinde bir sınır değere ulaşmaktadırlar. Bu şişme davranışı sadece kil konsantrasyonunun kritik bir değerin üzerinde olduğu durumlarda gözlenmektedir. Şişme ölçümlerini elastisite testleriyle birleştirilerek jellerin çapraz bağ yoğunluklarının, ν_e, öncelikle azadığı ardından, artan şişme süresiyle birlikte artış gösterdiği bulunmuştur. Çapraz bağ yoğunluğundaki bu değişim, kil miktarı artırıldığında veya kimyasal çapraz bağlayıcı oranı *X* azaltıldığında daha belirgin hale gelmektedir. Sonuçlar, şişme süresince iç içe geçmiş olan zincirlerin ve kil parçacıklarının yeniden düzenlenmesi ile açıklanmıştır. Ayrıca yapılan deneyler sonucunda, nanokompozit hidrojellerin seyreltik sulu aseton veya 10000 g/mol ağırlığındaki poli(etilen oksit) çözeltilerinde dağıldığı gözlenmiştir

1. INTRODUCTION

Polymeric gels are swollen crosslinked polymer networks that have both liquid-like and solid-like properties[1]. The liquid-like properties result from the fact that the major constituent of gels is usually a liquid while the solid-like properties result from the polymer network that holds the liquid and prevents it from flowing, like a cage. The properties of the gel depend strongly on the interaction of these two components.

When cross-linked polymeric materials are immersed in a good solvent, they absorb the liquid until the swelling force associated with the mixing entropy between the chains and the solvent balances the elastic force of the chains between junction points. These cross-linked polymeric systems containing the solvent are called gels [2].

Polymer gels can be prepared by chemical or physical crosslinking processes. Most of the gels are prepared by a chemical crosslinking process induced by free radicals, called free radical crosslinking polymerization. Here, a monovinyl monomer and a divinyl monomer (crosslinker) are copolymerized in the presence of a free radical initiator. On the other hand, physical gels can be obtained by hydrogen bonding, ionic interactions, miscellar interactions, clay-polymer interactions, etc.

Polymeric gels have a wide range of applications as ion-exchange resins, absorbents biomimetic materials, chemi-mechanical actuators, optical devices, drug delivery systems, etc. They are also used as molecular sieves, such as in gel permeation chromatography and electrophoresis [3].

However, application areas of hydrogels are quite limited as mechanical devices, due to their lack of mechanical strength. This weakness of gels originates from their liquid-like properties. Since the crosslinking polymerization reactions are carried out in an aqueous solution of the monomers, polymeric hydrogels formed are soft and very brittle when handled in the swollen state.

Several attempts have been made in recent years to design hydrogels with improved mechanical properties [4]. These can be categorized into three groups:

a. Topologic gels
b. Double network gels
c. Nanocomposite gels

Topologic gels:

Topological gels were synthesized recently from a polyrotaxane in which a poly(ethylene oxide) (PEO) chain with large molecular weight is sparsely populated with α-cyclodextrins[5]. By chemically cross-linking α-cyclodextrins contained in the polyrotaxanes in solution transparent gels with good tensility, low viscosity, and large swellability in water are obtained. Schematic representation of formation and structure of topologic gels is shown in Figure 1. In this gel, the polymer chains with bulky end groups are neither covalently cross-linked like chemical gels nor do they interact attractively like physical gels, instead they are topologically interlocked by figure-of-eight crosslinks (Fig. 1.1b and c). It is expected that these crosslinks can pass along the polymer chains freely to equalize the tension of the threaded polymer chains just like pulleys. Therefore, the nanoscale heterogeneity in structure and stress may be automatically equalized in the gel. This topological gel by figure-of-eight crosslinks is called as a polyrotaxane gel.

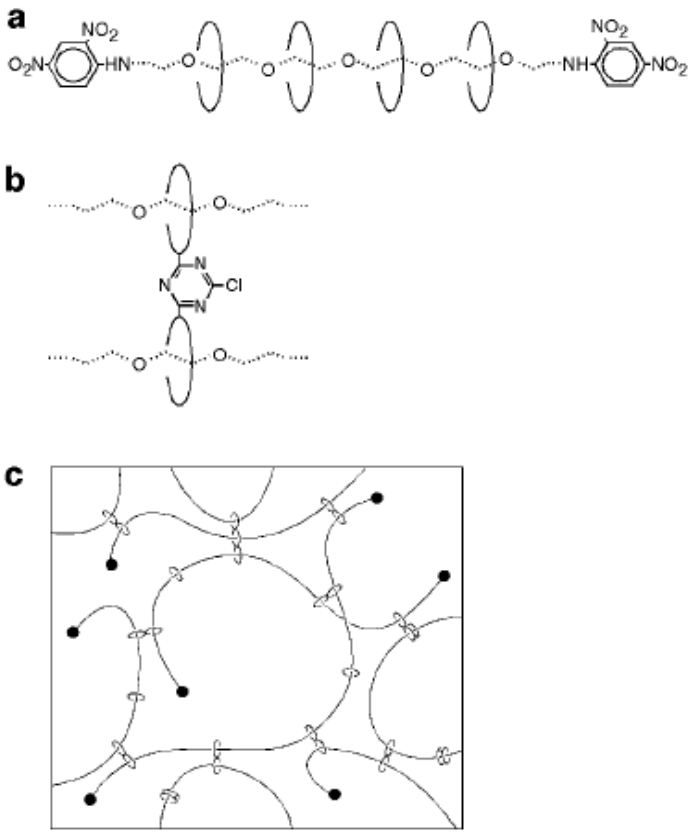

Figure 1.1: a) The polyrotaxane consisting of a-cyclodextrin and poly(ethylene oxide). b) The figure-of-eight crosslink: covalently crosslinked cyclodextrins. c) Schematic diagram of the polyrotaxane gel prepared from the sparse polyrotaxane by covalently cross-linking cyclodextrins. Cyanuric chloride can also cross-link between CD rings in the same polyrotaxane and three or more CDs.

Double network (DN) gels:

DN gels consist of two interpenetrating polymer networks: one is made of highly cross-linked rigid polymers and the other is made of loosely crosslinked flexible polymers (Figure 1.2). Such DN hydrogels with an optimized network structure can sustain a compressive pressure as high as several tens of megapascals [6].

A DN gel is synthesized via a two-step network formation process: the first step forms a highly cross-linked rigid gel, and the second forms a loosely cross-linked network in the first gel. An optimal combination is a poly(2-acrylamido-2-methylpropanesulfonic acid)

(PAMPS) gel as the first network and a poly(acrylamide) (PAAm) gel as the second network.

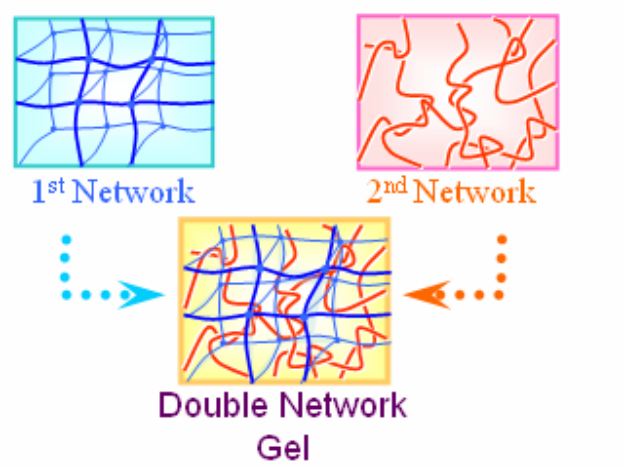

Figure 1.2: Schematic representation of a double network gel structure.

In conventional gels, mechanical stress applied is localized without effective dissipation. However, for the DN gels prepared at optimized conditions, mechanical stress is effectively and isotropically dissipated and this shows that loosely crosslinked second network effectively absorbs the crack energy by deforming the network conformation and/or sliding the physical entanglement points along the chains to prevent the crack growing to a macroscopic level. In other words, increased mechanical strength of DN gels is largely attributable to the effective relaxation of locally applied stress and dissipation of the crack energy through combinations of two networks with different structure densities [6].

Nanocomposite Hydrogels:

The nanoscale dispersion of layered silicates or clays in polymer networks is also one of the techniques offering significant enhancements in the material properties of hydrogels. Haraguchi et al. first prepared such hydrogels starting from acrylamide (AAm) - based monomers together with Laponite clay as a physical crosslinker, replacing the traditional

chemical crosslinker N,N-methylenebis(acrylamide) (BAAm) [7-10]. Laponite, a synthetic hectorite clay, when suspended in water forms disc-like particles with a thickness of 1 nm, a diameter of about 25 nm, and a negative surface charge density stabilizing dispersions in water [11,12]. The specific features of the nanocomposite hydrogels made using Laponite crosslinker is that both the clay particles and the polymer chains are of comparable size and, the lack of internal flexibility of the clay particles compared to the polymer chains. These features allow the clay particles to align easier than the polymer chains and leads to the improved mechanical properties of the hydrogels. Formation of a crosslinked polymer network using a small amount of Laponite indicates that these nanoparticles act as a multifunctional crosslinker with a large effective functionality [13]. Contrary to the conventional chemically crosslinked hydrogels, the nanocomposite hydrogels formed using Laponite as a crosslinker exhibit extraordinary mechanical toughness, tensile moduli, and tensile strengths [7-10]. Recently, it was observed by rheological experiments that large energy dissipation occurs during the deformation of the nanocomposite hydrogels that contain Laponite [14]. These results suggest that the polymer chains in the hydrogel are in a dynamic adsorption/desorption equilibrium with the clay particles, which is responsible for the excellent mechanical performance of these materials.

The goal of the present study was to explore the influence of specific clay-polymer interactions on the macroscopic properties of nanocomposite hydrogels. We investigated the equilibrium swelling behavior and the elastic properties of nanocomposite hydrogels. The nanocomposite hydrogels were prepared in aqueous solutions starting from acrylamide as the hydrophilic monomer and N,N'-methylenebisacrylamide (BAAm) as the chemical crosslinker in the presence of Laponite XLS as the clay component. As will be seen below, the properties of nanocomposite hydrogels differ from the conventional ones depending on the clay and the chemical crosslinker amounts, used in their preparation. The origin of this behavior is discussed on the basis of the results of the swelling and elasticity tests.

2. GENERAL PROPERTIES OF HYDROGELS

2.1. Swelling of Hydrogels

Polymeric gels absorb large quantities of suitable solvents without dissolving. As more and more solvent is absorbed by the polymer network, the network expands progressively. During the swelling process, the network chains are forced to attain more elongated conformation. As a result, like pulling a spring from both ends, a decrease in chain configurational entropy is produced by swelling. Opposing this, an increase in entropy of mixing of solvent with polymer accompanies the swelling.
The equilibrium swelling theory developed by Flory and Rehner treats polymer networks in the presence of small molecules. The theory considers forces arising from three sources:

1. The entropy change caused by mixing of polymer and solvent. The entropy change from this source is positive and favors swelling.

2. The entropy change due to the reduction in the number of possible chain conformations on swelling. The entropy change from this source is negative and opposes swelling.

3. The heat of mixing of polymer and solvent, which may be positive, negative or zero. Usually, it is slightly positive and opposing mixing.

In the following paragraphs, these forces are explained separately.

2.1.1 Entropy of Mixing in Polymer Solutions

Polymer solutions show deviation from the ideal solution behavior due to the fact that the molecular sizes of both polymer and solvent differ from each other. A special restriction on the arrangement of the two components in space resulted from the connectivity of polymeric chain segments. Flory [15, 16] and Huggins [17] expressed the total number of configurations of a mixture from N_1 solvent molecules with a molar volume V_1 and N_2 polymer chains with a molar volume V_2. In Fig. 2.1, the lattice theory suggested by Flory and Huggins is illustrated. Polymer chains are represented as consisting of x segments, each occupies one lattice site as a solvent molecule, i.e.,

$$x = V_2 / V_1 \tag{2.1}$$

The total number of lattice sites can thus be given as:

$$N_0 = N_1 + xN_2 \tag{2.2}$$

According to this theory N_2 polymer molecules are added one-by-one to the lattice before adding the solvent molecules. When adding a polymer, the first segment of the chain can be placed in any empty cell. However, for the connectivity required to represent a polymer molecule, each successive segment of remaining x-1 segment must be placed in any empty cell adjacent to the previously-placed segment. The individual numbers of possible placements are calculated for each segment of the chain and, by multiplying these numbers together, the total number (ν) of possible conformations of the polymer molecule in the lattice is obtained [18]. If i chains have already been inserted into the lattice, the number of possible conformations for the (i+1)th polymer molecule (ν_{i+1}) is given by:

$$\nu_{i+1} = \left\{ \frac{(N_0 - xi)!}{[N_0 - x(i+1)]!} \right\} \left[\frac{z-1}{N_0} \right]^{x-1} \tag{2.3}$$

where z is the coordination number of the lattice or the number of cells that are first neighbour to a given cell. The total number of distinguishable ways of placing the N_2 chains on $N_1 + xN_2$ sites is;

$$\Omega = \frac{1}{N_2!}\prod^{N_2-1}\nu_{i+1} \tag{2.4}$$

The number of ways Ω_2 by which chains can be placed on xN_2 sites is obtained by setting $N_1 = 0$ in Equation (2.4). The configurational entropy of mixing is;

$$\Delta S_m = k \ln \frac{\Omega}{\Omega_2} = -k\left[N_1 \ln \nu_1 + N_2 \ln \nu_2\right] \tag{2.5}$$

where ν_1 and ν_2 are the volume fractions of solvent and polymer defined as

$$\nu_1 = \frac{N_1}{N_1 + xN_2} \quad , \quad \nu_2 = \frac{xN_2}{N_1 + xN_2} \tag{2.6}$$

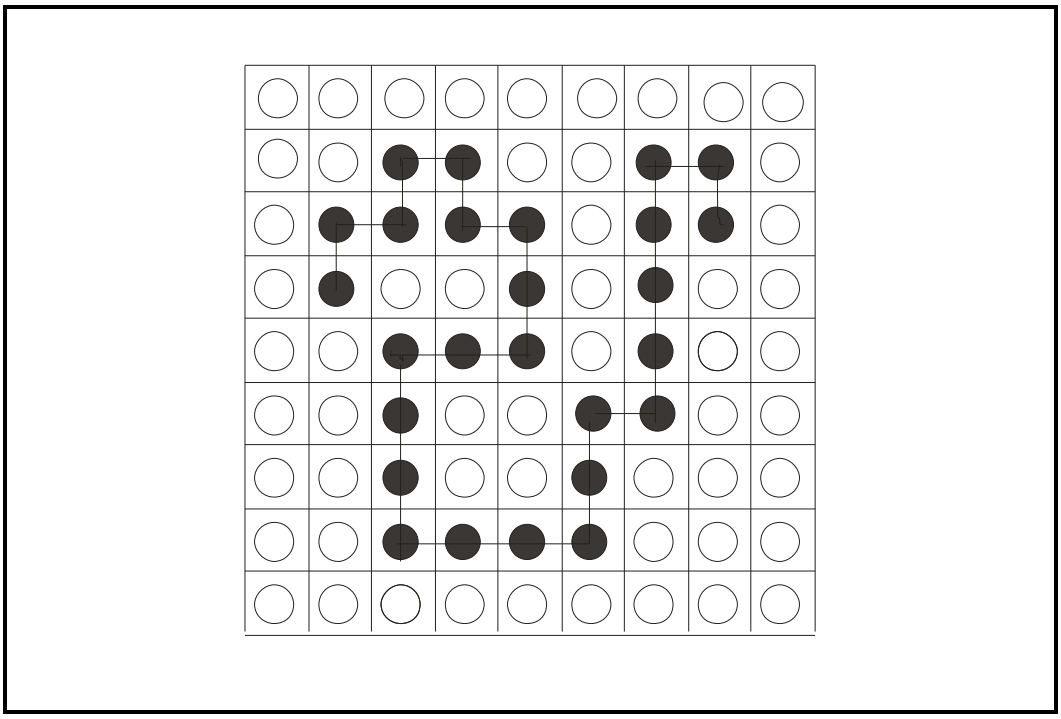

Figure 2.1: Lattice Theory suggested by Flory and Huggins. A part of the lattice consisting of a polymer chain is represented by filled symbols in the Figure. Open symbols represent solvent molecules [18].

2.1.2 Enthalpy and Free Energy of Mixing in Polymer Solutions

Solvent-solvent, segment-solvent and segment-segment interactions are possible within the same chain. The energies of these three types of interactions are represented by w_{11}, w_{12}, w_{22} respectively. The change in the internal energy for the formation of an unlike molecular pair is given by:

$$\Delta w = w_{12} - \frac{1}{2}\left(w_{11} + w_{22}\right) \tag{2.7}$$

and the expression for the enthalpy of mixing is given as:

$$\Delta H_m = zN_1\nu_2\Delta w_{12} \tag{2.8}$$

To eliminate z and Δw_{12} a parameter called Flory (or polymer-solvent) interaction parameter (χ_1) was introduced;

$$\chi_1 = \frac{z\Delta w_{12}}{kT} \tag{2.9}$$

The expression for the enthalpy of mixing was then rewritten by combining Equations (2.8) and (2.9) as follows:

$$\Delta H_m = kT\chi_1 N_1 \nu_2 \tag{2.10}$$

The quantity $kT\chi_1$ represents merely the difference in energy of a solvent molecule immersed in the pure polymer $(\nu_2 \cong 1)$ compared with one surrounded by molecules of its own kind, i.e., in the pure solvent.

The free energy of mixing can simply be obtained by combining equations (2.5) and (2.10):

$$\Delta G_m = kT\left[N_1 \ln \nu_1 + N_2 \ln \nu_2 + N_1 \chi_1 \nu_2\right] \tag{2.11}$$

2.2. Elasticity of Hydrogels

The understanding of the polymer network elasticity began in the early 1930s. The forms of the stress-strain relationships were developed beginning in 1942 with Wall [19], Treloar[20], Flory and Rehner[21], James and Guth[22]. The first molecular theory of rubber elasticity provided the first absolute prediction of mechanical modulus from network structure with the following assumptions:

- The polymer network contains v chains per unit volume.
- The mean square end-to-end distance for the chains consisting of N segments with each bond having a length l equals to $\langle r^2 \rangle = Nl^2$.
- There is no change of the volume on the deformation.
- The junction points between the chains move on deformation as if they were embedded in an elastic continuum. As a result of the components of length of each chain change in the same ratio as the corresponding dimensions.
- The entropy of the network is the sum of the entropies of the individual chains.

Elasticity of the polymer networks refers to two aspects: very high deformability and essentially complete recoverability. The crosslinked materials can undergo large deformations under tensions without rupturing. When the deforming force is removed, they spontaneously recover their original dimensions[23]. Three molecular requirements are needed to exhibit this type of elaticity:

1. the material must consist of polymer chains,
2. the chains must have a high degree of flexibility and mobility,
3. the chains must be joined into a network structure.

2.2.1 Statistical properties of long chain molecules

The statistical form of long-chain molecules may be illustrated by considering an idealized model of the polymethylene or paraffinic type of a chain $(CH_2)_n$ in which the

angle between successive bonds (i.e. the valence angle) is fixed but complete freedom of rotation of any given bond with respect to adjacent bonds in the chains is allowed. This is illustrated in Figure 2.2 in which the first two bonds C_1C_2 and C_2C_3 are represented as lying in the plane of the paper.

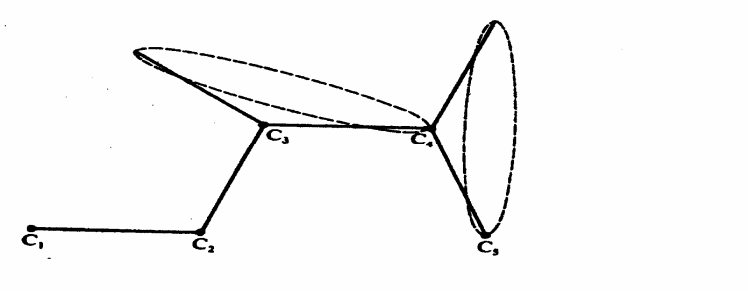

Figure 2.2: Rotation about bonds in paraffin-type molecule [20].

The third bond, C_3C_4 will in general not lie in this plane but will rotate in a random manner about the bond C_2C_3 as axis. Similarly C_4C_5 will rotate about C_3C_4, and so on. The chain will thus take up an irregular or randomly kinked form in which the distance between the ends is very much less than that corresponding to the outstretched or planar zigzag form (Figure 2.3).

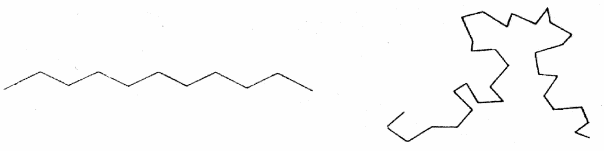

(a) (b)

Figure 2.3: (a) Planar zigzag; (b) randomly kinked chain.

The actual conformation will be subject to continual fluctuation due to thermal agitation and hence can not be defined explicitly, but it is possible to specify some of the properties of the system in statistical terms, or in terms of certain average values.

An idealized model for the development of the statistical theory consists of a chain of n links of equal lengths, l, in which the direction in space of any link is entirely random and bears no relation to the of any other link in the chain. Such a randomly jointed chain automatically excludes valence angle or other restrictions on the freedom of motion of neighboring links.

In order to define the statistical properties of the randomly jointed chain, one end (A) is assumed to be fixed at the origin of a Cartesian coordinate system O_x, O_y, O_z and the other end (B) moves in a random manner throughout the available space (Figure 2.4). However, although the motion is random, all positions of (B) are not equally probable. For any particular position p, having coordinates (x, y, z), there will be an associated probability that the end (B) shall be located within a small volume element (dxdydz=dτ). The derivation of this probability requires the evaluation of the relative numbers of configurations or conformations of the chain which are consistent with different positions of the point p, the probability of any particular position being taken as proportional to the corresponding number of conformations. The solution of this problem, given by Kuhn [24,25], Guth and Mark [26] is presented as:

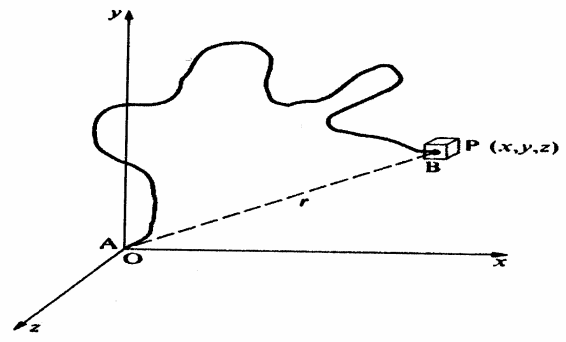

Figure 2.4: The statistically kinked chain. Specification of probability that the end should fall in volume element dτ (=dxdydz) [20].

$$p(x,y,z)dxdydz = \frac{b^3}{\pi^{1/2}} \exp(-b^2(x^2+y^2+z^2)dxdydz \quad (2.11)$$

where b is a constant and it is given by the following equation:

$$b^2 = 3/2nl^2 \quad (2.12)$$

and x, y, z are the components of the vector r, i.e.,

$$r^2 = x^2 + y^2 + z^2 \quad (2.13)$$

This formula gives the probability that the components of the vector r representing the end-to-end distance for the chain shall lie within the intervals x to x + dx, y to y+ dy, and z to z+dz, respectively. This probability is expressed as the product of the probability function p (x, y, z) and the size of the volume element considered, which in this case is dx dy dz(=dτ).

2.2.2 The entropy of a single chain

According to the general principles of statistical thermodynamics, as developed by Boltzmann, the entropy will be proportional to the logarithm of the number of conformations available to the system, i.e., to the logarithm of the number of possible conformations corresponding to any specified state. Thus, since the number of conformations available to a polymer chain is proportional to the probability density given by Equation (2.11) the entropy s of the chain is therefore given by:

$$s = k(\ln p(x, y, z)d\tau) \tag{2.14}$$

Substitution of the expression (2.11) for p(x,y,z) thus yields:

$$s = c - kb^2 r^2 \tag{2.15}$$

where c is an arbitrary constant which includes the volume element dτ. Equation (2.3) shows that the entropy has its maximum value when the ends of the chain are coincident ($r = 0$) and it decreases continuously with increasing distance between the ends.

2.2.3 The elasticity of a molecular network

The statistical theory of rubber elasticity is based on the concept of a network polymer as an assembly of long-chain molecules linked together at a relatively small number of points so as to form an irregular three-dimensional network. The statistical treatment of a network is similar in principle to the treatment of the single chain. It is required first to calculate the entropy of the whole assembly of chains as a function of the macroscopic state of strain in sample and form this to derive the free energy of work or deformation.

2.2.4 Entropy and free energy changes during deformation

Under an external strain, a unit cube (Figure 2.5) is transformed into a rectangular parallelepiped having three unequal edge lengths λ_1, λ_2, and λ_3. These extension ratios may be either greater than 1, corresponding to a stretched, or less than l, corresponding to a compression, provided that the condition for constancy of volume (assumption 3 above), namely:

$$\lambda_1 \lambda_2 \lambda_3 = 1 \tag{2.16}$$

is satisfied.

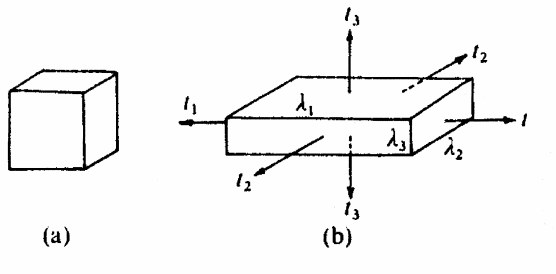

Figure 2.4: Pure homogenous strain (a) the unstrained state; (b) the strained state [25].

As seen in Figure 2.5, an individual chain in the unstrained state has an end to end distance r_o, with components (x_o, y_o, z_o). After deformation, the vector r_o becomes r and the components become (x, y, z). Then, the affine deformation assumption leads to the following equations:

$$\lambda_1 x_o, \qquad y = \lambda_2 y_o, \qquad z = \lambda_3 z_o \tag{2.17}$$

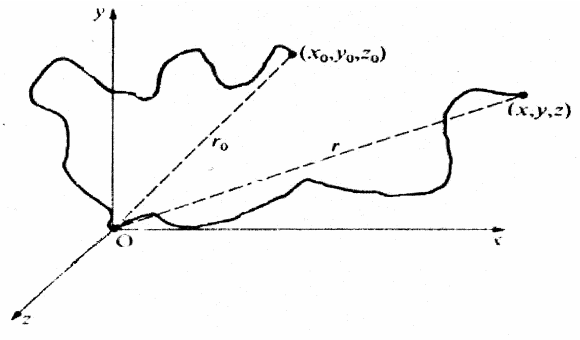

Figure 2.5: The affine deformation of a chain [25].

The entropy of the chain in the original (unstrained) state, as given by the equation (2.15), will be:

$$s_o = c - kb^2 r_o^{\,2} = c - kb^2 (x_o^{\,2} + y_o^{\,2} + z_o^{\,2}) \tag{2.18}$$

The entropy of the same chain in the strained state is obtained by substituting the values of (x, y, z) for (x_o, y_o, z_o), i.e.,

$$s = c - kb^2 (\lambda_1^{\,2} x_o^{\,2} + \lambda_2^{\,2} y_o^{\,2} + \lambda_3^{\,2} z_o^{\,2}) \tag{2.19}$$

The entropy change during deformation Δs_{el} will therefore be:

$$\Delta s_{el} = s - s_o = -kb^2 \left\{ (\lambda_1^{\,2} - 1) x_o^{\,2} + (\lambda_2^{\,2} - 1) y_o^{\,2} + (\lambda_3^{\,2} - 1) z_o^{\,2} \right\} \tag{2.20}$$

The total entropy for all the ν chains of the network is obtained by summation of the expression (2.20) for all the chains:

$$\Delta S_{el} = \sum_{i=1} \Delta s = -kb^2 \left\{ (\lambda_1^{\,2} - 1) \sum_{i=1}^{\nu} x_0^{\,2} + (\lambda_2^{\,2} - 1) \sum_{i=1}^{\nu} y_o^{\,2} + (\lambda_3^{\,2} - 1) \sum_{i=1}^{\nu} z_o^{\,2} \right\} \tag{2.21}$$

Since the directions of the chain vectors r_o in the unstrained state are entirely random, there will be no preference for the x, y, z directions. Thus, since:

$$\sum_{i=1}^{\nu} x_o^{\,2} + \sum_{i=1}^{\nu} y_o^2 + \sum_{i=1}^{\nu} z_o^2 = \sum_{i=1}^{\nu} r_o^2 \tag{2.22}$$

it may be written as:

$$\sum_{i=1}^{\nu} x_o^2 = \sum_{i=1}^{\nu} y_o^2 = \sum_{i=1}^{\nu} z_o^2 = \frac{1}{3}\sum_{i=1}^{\nu} r_o^2 \tag{2.23}$$

Furthermore, since the mean-square end-to-end distance of the chains $\overline{r_o^2}$ is defined as:

$$\overline{r_o^2} = \sum_{i=1}^{N} r_o^2 / \nu \tag{2.24}$$

Equation (2.21) can then be written :

$$\Delta S_{el} = -\frac{1}{3}\nu k b^2 \overline{r_o^2}\,(\lambda_1^2 + \lambda_2^2 + \lambda_3^2 - 3) \tag{2.25}$$

The assumption that the mean-square chain vector length in the unstrained state, $\overline{r_o^2}$ is the same as for a corresponding set of free chains, $\overline{r_o^2} = \frac{3}{2b^2}$ leads to the following equation:

$$\Delta S_{el} = -\frac{1}{2}\nu k(\lambda_1^2 + \lambda_2^2 + \lambda_3^2 - 3) \tag{2.26}$$

Assuming that there is no change of volume on deformation, the Helmholtz and Gibbs free energies of elastic deformation can be written using Equation (2.26) as:

$$\Delta A_{el} = -T\Delta S_{el} = \frac{1}{2}\nu kT(\lambda_1^2 + \lambda_2^2 + \lambda_3^2) \tag{2.27}$$

$$\Delta G_{el} = \Delta A_{el}$$

2.2.5 Mechanical Testing of Polymer Networks

Analysis of the deformation of the polymer network resulting from the application of a stress is one of the important ways to characterize the polymer networks. The results are generally expressed in terms of the stress *f* and the strain α, so as to be independent of sample geometry. Stress is the force acting per unit original cross-sectional area and its unit is Newtons per square meter (Nm^{-2}), i.e., pascal (Pa). Strain is the deformation per unit original dimension and is therefore dimensionless. The ratio of stress to strain is called the modulus.

The experimental studies are generally based on the measurements of uniaxial deformation, particularly on the measurements of simple compression or elongation.

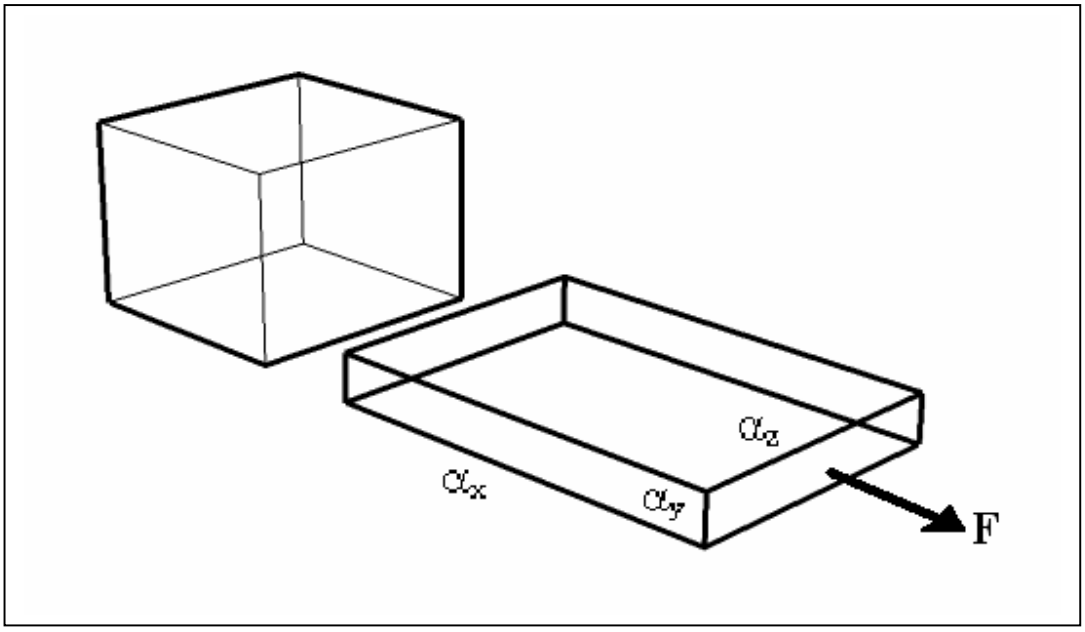

Figure 2.6: The uniaxial deformation of polymer network.

Equation (2.27), i.e., $\Delta G_{el} = \frac{1}{2}\nu kT\left(\alpha_1^{\,2} + \alpha_2^{\,2} + \alpha_3^{\,2} - 3\right)$ is general and can be used to obtain the stress-strain relationship for any type of the deformation. Its application is the best illustrated in the great majority of the experimental studies.

In the polymer network, applying a force in one direction can cause deformations in other directions. Consider that a cubic polymer network sample is subjected to a constant uniaxial stress to derive a stress-strain equation. As shown in Figure 2.6, under such a stress, the cubic polymer network is transformed into a rectangular parallelepiped having three edge length. The deformation ratios α_x, α_y, and α_z which are obtained directly from the dimensions of the polymer network in the strained state and in the (initial) unstrained state, equal to $(L/L_0)i$, where $i = x, y,$ or z. These extension ratios may be either greater than 1, corresponding to a stretch, or less than 1, corresponding to a compression. This deformation occurs at essentially constant volume can be formulated as follows:

$$\lambda_1 \lambda_2 \lambda_3 = 1$$

In the previous section, an equation describing the changes in the entropy ΔS_{el} was presented. Assuming that there is no change of volume on deformation, the Gibbs or Helmhotz free energies of elastic deformation can be written:

$$\Delta G_{el} = \Delta A_{el} = -T\Delta S \tag{2.16}$$

Since work of deformation W equals to ΔA_{el}, using Equation (2.16), the following equation for W can be written:

$$\Delta G_{el} = \frac{1}{2}\nu kT\left(\alpha_1{}^2 + \alpha_2{}^2 + \alpha_3{}^2 - 3\right) \tag{2.17}$$

For uniaxial deformation, since $\alpha_2{}^2 = \alpha_3{}^2 = \frac{1}{\alpha}$ and $\alpha_1{}^2 = \alpha^2$, Equation (2.17) reduces to:

$$W = \frac{1}{2}\nu kT\left(\alpha^2 + \frac{2}{\alpha} - 3\right) \tag{2.18}$$

where α is the linear deformation ratio (deformed length/initial length) due to the applied force F on the gel sample. By using Equation (2.18), the force F acting on the gel sample can be calculated:

$$F = \left(\frac{\partial W}{\partial \alpha}\right)_{T,V} = \frac{1}{2}\nu kT\left(2\alpha - \frac{2}{\alpha^2}\right) = \nu kT\left(\alpha - \frac{1}{\alpha^2}\right) \tag{2.19}$$

Equation (2.19) involves a single physical parameter νkT, which is only dependent on the crosslink density of the material. This is called the elastic modulus G of the gel in dried state:

$$G_{dry} = \nu kT = \frac{\rho}{Mc}RT \tag{2.20}$$

As the gel swells, the elastic modulus decreases due to the decrease in the concentration of the network chains ν. The elastic modulus of swollen gels is given by the following equation:

$$G = A\frac{\rho}{Mc}RT\left(\nu_2{}^0\right)^{2/3}\left(\nu_2\right)^{1/3} \tag{2.21}$$

where R is gas constant and T is temperature. The front factor A equals to 1 for an affine network and $1-2/\Phi$ for a phantom network, where Φ is the functionality of the crosslinks.

Since $\nu_2{}^0 = \nu_2$ for the hydrogels just after preparation, the modulus G_0 after preparation becomes:

$$G_0 = A\frac{\rho}{Mc}RT\nu_2{}^0 \tag{2.22}$$

2.2.6 Factors affecting the elastic modulus of polymer networks

i. **Network structure:** The stiffness of the polymer backbone of the gels affect the elastic modulus. A gel consisting of stiff network chains due to the bulky side group is expected to have higher elastic modulus than a flexible polymer.

ii. **The initial monomer concentration:** As the monomer concentration is increased, the effective crosslink density v_e of the hydrogels also increases due to the more efficient consumption of the crosslinker molecules in concentrated monomer solutions, so that the elastic modulus of gels becomes larger.

iii. **The crosslinker concentration:** The elastic mdulus of gels sensitively depends on the crosslinker concentration. The modulus of gels increases with

increasing crosslinker concentration due to decreasing chain length between successive crosslinks.

iv. **Structral heterogeneities:** The elastic modulus of gels also depends on the sample location, at which the mechanical measurements are carried out. It was shown that the modulus G_0 increases continuously with increasing distance from the bottom of the gel rod, indicating that the effective crosslink density of the network chains increases along the same direction within the gel. It was also shown that the modulus decreases as the degree of the structural heterogeneity increases[27].

v. **Ionic group concentration:** The elastic modulus of gels after their preparation first increases with increasing charge density but then decreases continuously[28,29]. The results indicate two opposite effects of charged groups on the elastic modulus of hydrogels: Formation of multiplets in the gel increases the elastic modulus of ionic hydrogels, whereas the effect of the elctrostatic interaction of charged groups on elastic free energy decreases the modulus.

3. CLAY MINERALS

Clays represent one of the traditional materials, whose applications have played an important role throughout human history [30]. They find very fundamental uses in human life, such as building materials, ceramics, rheology modification, catalysis, paper filling, etc. [31]. With the availability of customized synthetic clays, there is a growing scientific activity associated with including clays into modern materials science together with other synthetic and complex adaptive materials such as colloids, polymers, liquid crystals, biomaterials, etc. [32].

Clay minerals are hydrous aluminum silicates and are generally classified as phyllosilicates with a two dimensional sheet-like structure, or layered silicates. Framework layers of natural clays are generated by a combination of tetrahedral and octahedral sheets. Silica is the main component of a tetrahedral sheet whilst octahedral sheet comprises diverse elements such as Al, Mg, and Fe. A natural stacking of tetrahedral and octahedral sheet occurs in the specific ratios and modes, leading to the formation of the 2:1 and 1:1 layer silicates.

2:1 layered silicates are the most important class of clays in terms of industrial applications, due to their swelling properties. However it is the non-swelling, 1:1 clays one usually encounters in the “ground" and in ceramics. In 2:1 layered silicates octahedral sheet is sandwiched between two tetrahedral sheets where in 1:1 layered silicates, there is only one tetrahedral structure linked to the octahedral. The phyllosilicate 2:1 layer clays include mica, smectite, vermiculite, and chlorite. Smectite group can be further divide into montmorillonite (MMT), bentonite, saponite, hectorite and Laponite species [33].

A schematic representation of smectite clays is shown in Figure 3.1. The tetrahedral sheet of smectites is composed of corner-linked tetrahedral, whose central ions are Si^{4+}

or Al^{3+} and sometimes Fe^{3+}. The basal oxygens of a tetrahedron are shared by the neighboring tetrahedral, forming hexagonal pattern. Thus the crystal lattice of 2:1 phyllosilicate consists of 1 nm thin layers, with an octahedral alumina sheet sandwiched between two tetrahedral silica sheets. The stacking of the platelets leads to a Van der Walls gap or so-called gallery between the platelets.

The layer charge can easily be generated by the replacement of cations in the alumina sheet with cations of different charges. Replacement of Al^{3+} by Mg^{2+} or Fe^{2+} produces negatively charged layers. This negative charge is balanced by alkali cations (Na^{+}, Li^{+} or Ca^{2+}) positioned in the gallery between the aluminosilicate layers.

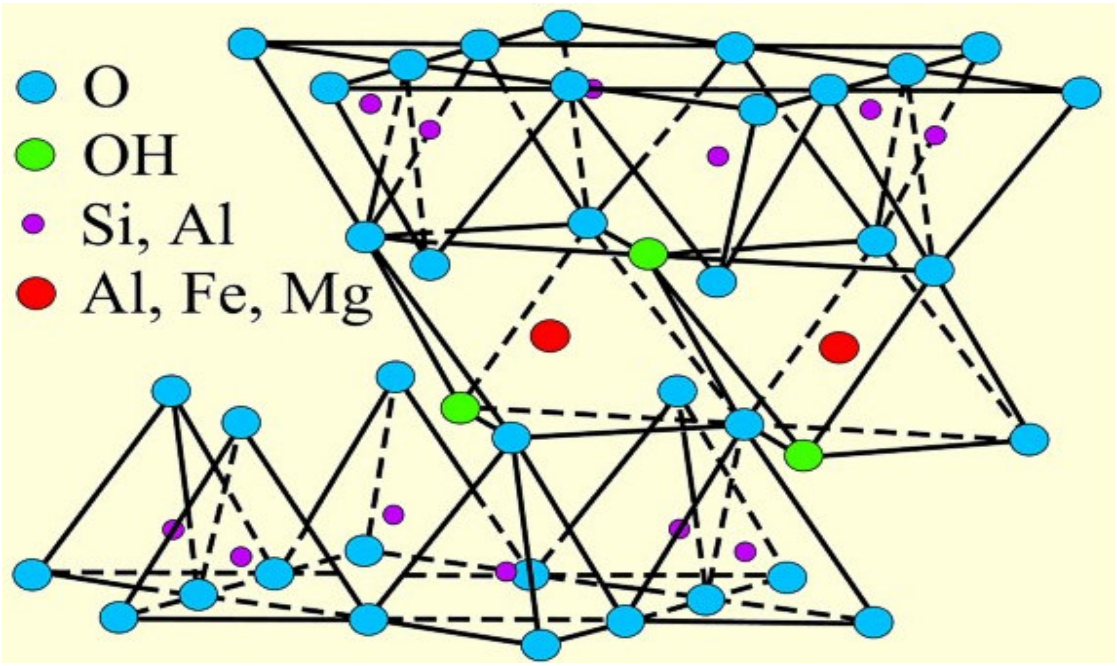

Figure 3.1: Schematic representation of a clay mineral

3.1. Laponite

Laponite, a subgroup of smectite family, is a synthetic smectite clay which is hydrous sodium lithium magnesium silicate. Single Laponite crystal has a diameter of 25 nm and thickness of approximately 1 nm. Laponite is in the form of disc-shaped crystals when dispersed in water. It can be seen as a two-dimensional inorganic polymer where the empirical formula is $Na^{0.7+}[(Si_8Mg_{5.5}Li_{0.3})O_{20}(OH)_4]^{0.7-}$. The edges of the crystal have small localised positive charges generated by absorption of hydroxyl groups where the crystal structure terminates. The unit cell is repeated many times in two directions, resulting in the disc-shaped appearance of the crystal shown below in Figure 3.2. [34]

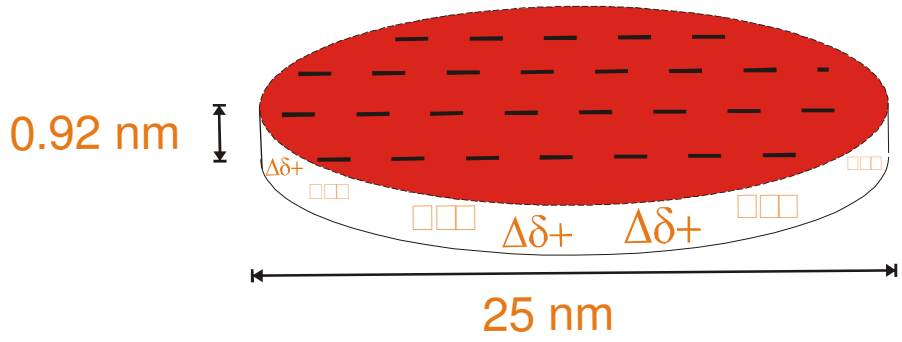

Figure 3.2: Schematic representation and dimensions of a single Laponite clay disc

The negative charge becomes neutralized during drying as sodium ions are absorbed onto the surfaces of the crystals. In solid state, the crystals become arranged into stacks which are held together electrostatically by sharing of sodium ions in the interlayer region between adjacent crystals. The processes occurring during dispersion of Laponite into water are shown schematically in Figure 3.3.

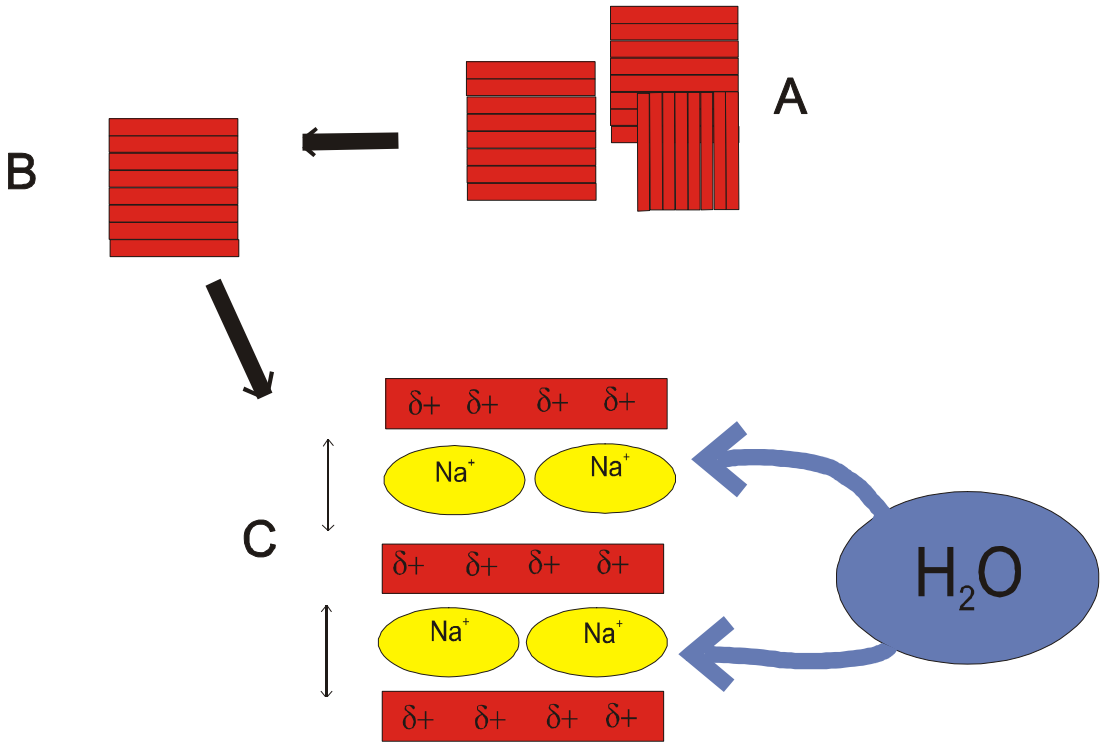

Figure 3.3: Schematic representation of the swelling process of Laponite. A) Aggregated particle stacks, B) Individual particle stacks C) Swelling of the platelets

Electrostatic attractions draw the sodium ions in solution towards the crystal surface and osmotic pressure from the bulk of water pulls them away. An equilibrium becomes established where the sodium ions are held in a diffuse region on both sides of the dispersed Laponite crystal as shown in Figure 3.3. These are known as electrical double layers.

When two particles approach their mutual positive charges repel each other and the dispersion exhibits low viscosity and Newtonian type rheology. The addition of polar compounds (e.g., simple salts, surfactants, coalescing solvents, soluble impurities and additives in pigments, fillers or binders etc.) to the dispersion of Laponite will reduce the osmotic pressure holding the sodium ions away from the particle surface.

This causes the electrical double layer to thin and allows the weaker positive charge on the edge of the crystals to interact with the negative surfaces of adjacent crystals. The process may continue to give a "house of cards" structure, that is shown in Figure 3.4, a highly thixotropic gel. This gel consists of a single flocculated particle held together by weak electrostatic forces.[34]

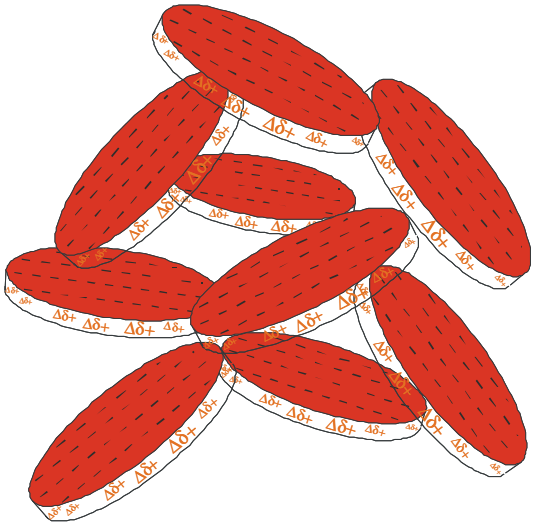

Figure 3.4: Thixotropic house of cards structure formed by Laponite

Laponite is the most widely studied synthetic clay until now [35]. What makes Laponite a particularly interesting model system is its nanometer sized dimensions and the mono dispersity of the colloidal platelets, in contrast to natural and other synthetic clays which in general are polydisperse and micrometer sized. Figure 3.5 showes the comparison of Laponite with two of the most widely used clay minerals, hectorite and bentonite [32].

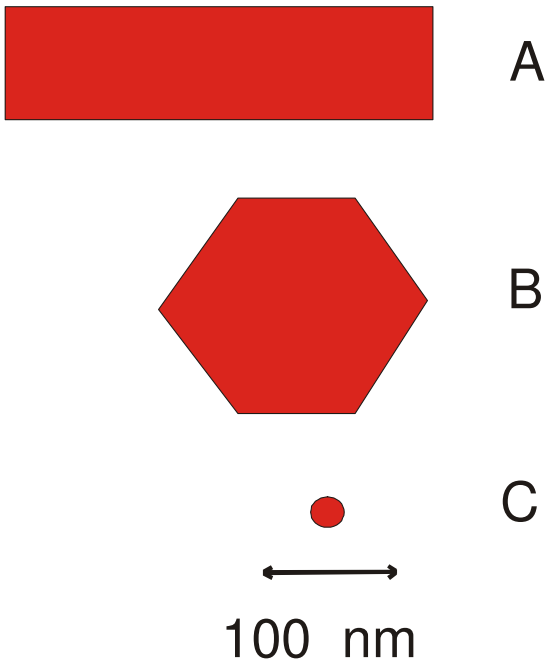

Figure 3.5: Size comparision of different clay particles. A) Hectorite clay, B) Bentonite clay, C) Laponite clay

4. POLYMER NANOCOMPOSITES

A ‘nanocomposite’ is defined as a particle-filled matrix in which at least one dimension of the dispersed phase is in the nanometer scale [36]. Polymer nanocomposites (PNC) are polymers (thermoplastics, thermosets or elastomers) that have been reinforced with small quantities (less than 5% by weight) of nano-sized particles having high aspect ratios (L/h > 300) [37]. They respresent a new class of material alternative to conventional filled polymers. In this new class of material, nanosized inorganic filler (at least one dimension) are dispersed in polymer matrix and provide improvements such as high moduli [38], increased strength and heat resistance [39], decreased gas permeability and flammability [40,41], and increased biodegradability of biodegradable polymers [42].

PCN were invented in 1985 at Toyota Central R&D Labs, Inc. (Toyota) [43]. It bore a new concept of polymer nanocomposites, expanded the field of polymer science including preparation, structure and interfaces and led to new applications for automotive, electric and food industries. Passenger cars equipped with a PCN part were launched in 1989, only 4 years after this discovery. Since then, extensive worldwide research on PCN has been conducted not only in the industrial sector but also in the academic sector.

PCN take advantage of smectite clays because of their swelling properties, high cation exchange capacities, high aspect ratio, and large surface areas [44, 45]. In general, layered silicates have layer thickness on the order of 1 nm and a very high aspect ratio (e.g. 10–1000). A few weight percent of layered silicates that are properly dispersed throughout the polymer matrix thus create much higher surface area for polymer/filler interaction as compared to conventional composites. There are three principal methods for synthesis of such nanocomposites: solvent methods, polymer melt intercalation and in situ polymerization. In solvent and melt intercalation, diffusion into the galleries

occurs from a solvent or the melt, respectively. In in situ polymerization, polymerization of monomers or oligomers takes place within the galleries [46].

The clays utilized in these composites belong to the smectite family. These clay are characterized by a 2:1 structure built of a central layer of octahedrally coordinated metal, normally Al^{3+} or Mg^{2+}, sandwiched between two tetrahedral coordinated layers of silicon. The morphology of these platy materials is characterized by a thickness of one nanometer. The two other dimensions are in the range of 100–1500 nanometers. The surface area of individual plates is greater than 750 m^2/g. This large surface area and aspect ratio dominate the interaction of these materials with polymers. Clays require surface modification for compatibility with a polymer of interest[46].

Isomorphous substitution in the crystal structure of these clays is common. In montmorillonite, the most common commercial nanoclay, the octahedral metal layer contains Al^{3+} which is replaced by Mg^{2+} or Fe^{2+}. Isomorphous substitution results in a charge imbalance in the structure. This is compensated by exchangeable cations on the surface of the clay plate. The exchangeable cation is normally sodium, potassium, calcium, or magnesium. The clay is normally very hydrophilic and will disperse into aqueous solutions forming thixotropic gels. This hydrophilic character makes them suitable for polymer systems that are water soluble or dispersable such as poly(vinyl alcohol), poly(ethylene oxide) or poly(acrylamide)[46].

5. EXPERIMENTAL PART

5.1. Materials and Chemicals

5.1.1 Monomers

Acrylamide (AAm, Fluka) was used as monomer without any purification. It's molecular weight is 71.08 g/mol.

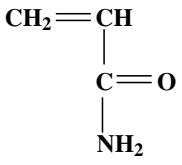

AAm

N,N'-methylenebisacrylamide (BAAm, Fluka) was used as crosslinking agent in the polymerizations and used as received. Its molecular weight is 154.17 g/mol.

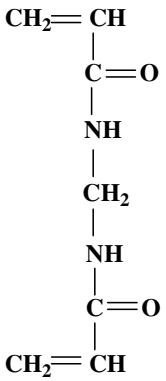

BAAm

Laponite XLS : The synthetic hectorite clay, Laponite XLS, ($Na^{0.7+}[Si_8Mg_{5.5}Li_{0.3})O_{20}(OH)_4]^{0.7-}$) modified with pyrophosphate ions ($(P_2O_7)^{4-}$) was provided by Rockwood Ltd. Note that both the surfaces and the edges of Laponite XLS discs are negatively charged, leading to electrostatic repulsion among the discs and efficiently prohibiting the formation of a gel structure [11, 12]. Indeed, Laponite XLS can be easily dispersed in water up to about 10 % concentration. Suspensions of Laponite XLS were prepared by dispersing the white powder at the preset concentrations in deionized water with vigorous stirring for one week.

5.1.2 Redox-initiator system

N,N,N',N'- tetramethylethylenediamine (TEMED, Carlo Erba) was used as stock solution. Its molecular weight is 116.21 g/mol.

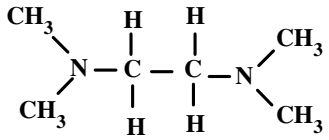

TEMED

Ammonium persulfate ($(NH_4)_2S_2O_8$, APS, Merck) was used as received. Its molecular weight is 228.20 g/mol.

5.1.3 Solvent

Distilled water was used for synthesis of the hydrogels, for swelling and reswelling processes.

Acetone was used for deswelling processes.

Poly(ethylene oxide) (PEO, Fluka) was used as the solute in the swelling experiments and it is used as received. Its molecular weight is 10000 g/mol.

5.2. Experimental Set-up and Equipment

5.2.1 Electronic Balance

The electronic balance of Precisa 205A was used in the experiments. It displays to four decimal places and its weighting capacity is 205 g.

5.2.2 Temperature-Sensitive Oven

The oven (Nüve EN 400) is used to supply environmental temperature condition (50 ^{o}C). It runs in range of 0 - 80 ^{o}C with the sensitivity of 1 ^{o}C.

5.2.3 Digital Compass

The diameters of the cylindrical gel samples were measured using a calibrated digital compass (Mitutoyo). The device has a measuring range between 0-150 mm with an accuracy ± 0.02 mm.

5.2.4 Tubes and Syringes

Gelation experiments were carried out in both glass tubes and plastic syringes with 10 cm long, 3.90-4.05 mm and 4.5 - 4.6 mm internal diameter respectively.

5.2.5 Uniaxial Compression Apparatus

In order to measure mechanical properties of the gel samples, a home-made uniaxial compression apparatus was used. This apparatus is consisted of three parts as shown in Figure 5.1. A digital comperator is sensitive to displacements of 10^{-3} mm and the balance is from Sartorius (IDC type Digimatic Indicator 543-262, Mitutoyo).

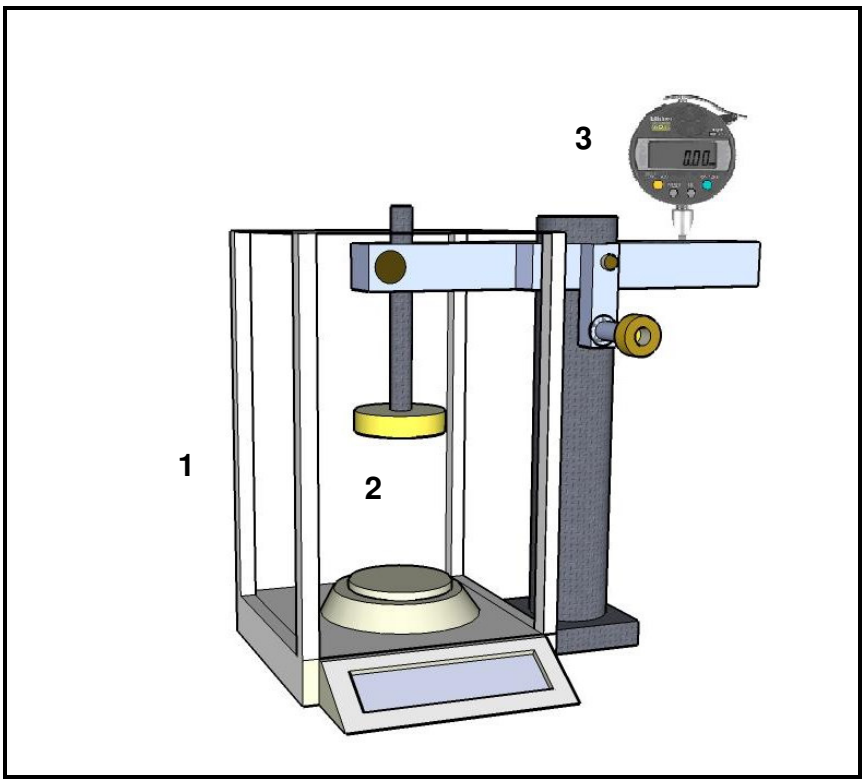

Figure 5.1: Apparatus for carrying out stress-strain measurements. 1. Digital electronic balance, 2. PTFE coated piston and 3. Digital comparator.

5.2.6 Monitoring of the Swelling Behavior of the Gels

The swelling behavior of the nanocomposite hydrogels was investigated by an optical microscope conducted with a PC. The gel samples were immersed into excess amount of distilled water and the change in volume swelling ratio is followed by the photographs taken periodically in every hour. Photographs taken from the gels were captured by Q Imaging Camera, MicroPublisher 3.3 RTV connected to PC, and analysed with software Image-Pro PlusVersion 6.0. The image analysing system is shown in figure 5.2.

Figure 5.2: Image analysing system

5.3. Experimental Procedure

5.3.1 Synthesis of PAAm-Laponite Nanocomposite Hydrogels

The gels consisting of different Laponite contents were prepared by free radical crosslinking copolymerization of AAm and BAAm in Laponite dispersions. Distilled water was used as the polymerization solvent. The reactions were initiated using TEMED (0.25 ml / 100 ml reaction solution) and APS (0.0035 M) redox initiator system.

The initial monomer (AAm) concentration was fixed at 5 % (w/v). BAAm was used as the chemical crosslinker of the nanocomposite hydrogels.

Mainly, two sets of nanocomposite hydrogels were prepared. In the first set, the chemical crosslinker ratio *X* (mole ratio of crosslinker BAAm to monomer AAm) was fixed at 1/80 while the Laponite concentration in the reaction system was varied between 0 and 7 w/v % (Table 1). In the second set, the Laponite concentration was fixed at 7 w/v % while the crosslinker ratio was varied between 1/1000 and 1/80 (Table 2).

General synthetic procedure for the experiments in details is given below:

The monomer AAm, crosslinker BAAm and the accelerator TEMED (0.25 v/v %) were first dissolved in Laponite XLS aqueous suspensions. After bubbling nitrogen, the initiator APS (3.51 mM) was added to the reaction solution and the polymerization was carried out in glass tubes and plastic syringes of about 4 and 4.5 mm internal diameter respectively for 24h. In this way, several series of PAAm nanocomposite hydrogels were prepared at various clay contents.

After polymerization, the tubes and syringes were taken out of the place which were supplied the reaction condition. The crude hydrogels were freed and they were cut into the samples of about equal length. After the compression test, each sample was then placed in distilled water at room temperature to swell.

Table 1. Feed composition for the synthesis of PAAm – Laponite nanocomposite hydrogels at various Laponite XLS contents (total reaction volume is 10 mL)

Laponite XLS (g)	AAm (g)	BAAm (g)	APS (g)	TEMED (ml)	Laponite XLS % (w/v) content
0	0.487	0.013	0.008	0.025	0
0.1	0.487	0.013	0.008	0.025	1
0.2	0.487	0.013	0.008	0.025	2
0.3	0.487	0.013	0.008	0.025	3
0.4	0.487	0.013	0.008	0.025	4
0.5	0.487	0.013	0.008	0.025	5
0.6	0.487	0.013	0.008	0.025	6
0.7	0.487	0.013	0.008	0.025	7

Table 2. Feed composition for the synthesis of PAAm – Laponite nanocomposite hydrogels at various crosslinker contents (total reaction volume is 10 mL).

BAAm (g)	Mol % of BAAm to Aam monomer	Aam (g)	APS (g)	TEMED (ml)	Laponite XLS (g)
0.013	1.25	0.487	0.008	0.025	0.7
0.005	0.50	0.495	0.008	0.025	0.7
0.002	0.20	0.498	0.008	0.025	0.7
0.001	0.10	0.499	0.008	0.025	0.7

5.4. Characterization Methods

5.4.1 Equilibrium Swelling Measurements

The nanocomposite hydrogels formed in glass tubes and plastic syringes of about 4 and 4.5 mm internal diameter respectively were cut into samples of about 10 mm length. Then, each sample was placed in an excess of water at 25 °C. In order to reach swelling equilibrium, the hydrogels were immersed in water for 1 month, replacing water several times. The swelling equilibrium was tested by measuring the diameter of the gel samples by a digital compass. To achieve good precision, five measurements were carried out on samples of different length taken from the same gel.

Swelling measurements were also carried out in aqueous NaCl solutions, acetone – water mixture and PEO solutions at various concentrations. For the swelling measurements in NaCl solutions, NaCl concentration is varied from 10^{-5} to 1.0 M. The hydrogels equilibrium swollen in water were transferred to vials containing the most diluted aqueous NaCl solution. The gel samples were allowed to swell in the solution for 2 weeks, during which aqueous NaCl was refreshed to keep the concentration as needed. After the swelling equilibrium is established, the gel samples were transferred into the next concentrated NaCl solution.

The swelling ratios of the hydrogels were measured by using volumetric techniques. For volumetric measurements, the diameters of the gel rods after preparation (D_o) and after

swelling (D) were measured by the calibrated digital compass. The equilibrium swelling ratio of the gel samples with respect to the after preparation state was calculated as

$$volume\ swelling\ ratio\ (V_{rel}) = \frac{V}{V_o} = \left(\frac{D}{D_o}\right)^3 \quad (5.1)$$

For gravimetric measurements, the weights of the gel rods after preparation (m_o) and after swelling (m_{sw}) were measured by the electronic balance. The equilibrium weight swelling ratio of the gel samples with respect to the after preparation state was calculated as

$$\text{Weight swelling ratio } (m_{rel}) = \frac{m_{sw}}{m_o} \quad (5.2)$$

5.4.2 Mechanical Measurements

Uniaxial compression measurements were performed on hydrogels after their preparation state as well as at various states of swelling in water. All the mechanical measurements were conducted in a thermostated room, 25 ^oC.

Briefly, cylindrical gel sample after preparation was placed on the electronic balance. A load was transmitted vertically to the gel through a rod fitted with a PTFE (Teflon) end-plate. The force acting on the gel was calculated from the reading of the balance m as F=mg, where g is gravitational acceleration. The resulting deformation $\Delta\ell = \ell_o - \ell$, where ℓ_o and ℓ are the initial undeformed and deformed lengths, respectively. The force and the resulting deformation were recorded after 20 sec of relaxation. The measurements were conducted up to about 20 % compression. The deformation ratio α (deformed length / initial length) was calculated as $\alpha = 1 - \Delta\ell/\ell_o$. The corresponding f was calculated as f = F / A, where A is the cross-sectional area of the specimen, $A=\pi(Do/2)^2$, where D_o is its initial diameter.

The elastic modulus G_0, in after preparation state and G, at various states of swelling was determined from the slope of the linear dependence of stress-strain isotherms by using the equation

$$f = G (\alpha - \alpha^{-2}) \qquad (5.5)$$

6. RESULTS AND DISCUSSION

The main purpose of this study was to determine the effect of Laponite on the swelling properties and the elastic behavior of polyacrylamide (PAAm) nanocomposite hydrogels. To understand the crosslinker effect of Laponite, the gelation reactions of acrylamide (AAm) monomer were carried out in the presence of varying amounts of Laponite. The chemical crosslinker N,N'-methylenebis(acrylamide) (BAAm) was also used in the preparation of the nanocomposite hydrogels to compare the relative contributions of the chemical and physical crosslinks. Three sets of experiments were carried out:

In the first set of experiments, the elastic behavior and the swelling capacities of the nanocomposite hydrogels containing various amounts of Laponite were investigated. In this set of experiments, both the monomer (AAm) concentration and the chemical crosslinker ratio (molar ratio BAAm/AAm) were fixed at 5 w/v % and 1/80, respectively.

In the second set, the properties of the nanocomposite hydrogels were investigated at a fixed Laponite content of 7 w/v % but at various chemical crosslinker ratios.

In the third set, the elastic and swelling behaviors of the nanocomposite hydrogels in acetone-water mixtures, in aqueous PEO solutions as well as in aqueous salt solutions were investigated.

6.1. Laponite dispersions

Before we discuss the characteristics of (PAAm)/Laponite nanocomposite hydrogels, it is appropriate to obtain some view of the corresponding primary system, namely the

pure Laponite dispersions. Laponite clay has a structural negative charge which is neutralized by the Na^+ ions absorbed onto the surfaces of the crystals. As schematically illustrated in Figure 6.1 (A), the crystals in the solid state become arranged into stacks, which are held together electrostatically by sharing of Na^+ ions in the interlayer region between adjacent crystals. When dispersed in water, Laponite stacks gradually cleave into discrete disc-like particles. In aqueous dispersions, electrostatic attractions draw the Na^+ ions towards the negatively charged particle surface, while the osmotic pressure from the bulk of water pulls the Na^+ ions away from the particle surface. An equilibrium becomes established where the Na^+ ions are held in a diffuse region on both sides of the dispersed Laponite particles. This electrical double layer causes the particles to repel each other so that dispersions of Laponite are stable at low concentrations (Figure 6.1 (B)).

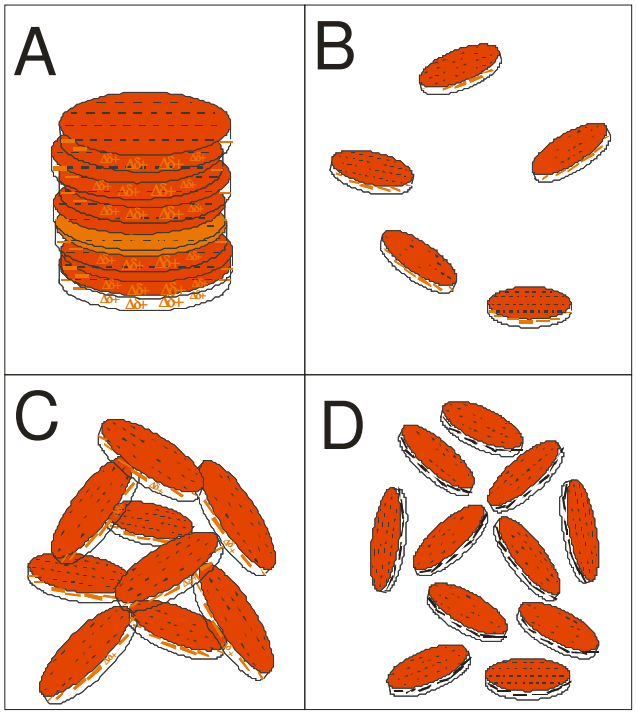

Figure 6.1: Schematic representation of Laponite clay in various forms. (A) In dry state, (B) In dispersed state with a large amount of water, (C) In a gel state with a "House of cards" structure, and (D) In dispersed state at a high Laponite concentration after treatment with pyrophosphate anions.

However, increasing the Laponite concentration above 2 %, or addition of polar compounds such as salts, surfactants, or ionic monomers to the Laponite dispersions reduces the osmotic pressure holding the Na^+ ions away from the particle surface. This causes the electrical double layer to thin and allow the positive charge on the edge of the particles to interact with negative surfaces of adjacent particles. This results in the formation of a "House of cards" structure and the dispersion system becomes a highly thixotropic gel [34] (Figure 6.1 (C)). However, the binding between the negatively charged face and the positively charged edge of the Laponite particles can be inhibited by the addition of pyrophosphate ions [12]. In this case, the edges of the Laponite discs modified by pyrophosphate are negatively charged so that the surfaces and edges of discs exhibit the same charge, leading to electrostatic repulsion among the discs and efficiently prohibiting the formation of a gel structure (Figure 6.1 (D)).

In the present work, we used Laponite XLS, a Laponite clay modified with pyrophosphate ions. Therefore, Laponite XLS can be easily dispersed in water up to about 10 % concentration. When Laponite XLS powder is added to water and vigorously shaken, an initially opaque suspension is formed and, at concentrations below 5 w/v % Laponite, the suspension becomes completely transparent in a few hours.

6.2. Effect of Laponite concentration on the properties of nanocomposite hydrogels

After formation of stable Laponite dispersions, the monomer AAm, the chemical crosslinker BAAm and the redox initiator system APS/TEMED were added into the dispersion and the free-radical crosslinking copolymerization was conducted at 5°C. In this section, a series of nanocomposite PAAm hydrogels with various amounts of clay (Laponite) were prepared. The initial monomer (AAm) concentration was set to 5 w/v %. The chemical crosslinker ratio *X*, that is, the molar ratio of the crosslinker BAAm to the monomer AAm was also fixed at 1/80 while the clay content in the reaction mixture was varied between 0 – 7 w/v %.

In Figure 6.2, the elastic moduli G_o of the hydrogels just after their preparation are shown as a function of the Laponite content of the reaction solution. It is seen that the

modulus of elasticity first increases with the addition of 1 % Laponite but then remains constant up to 4%; at higher Laponite concentrations, the elastic modulus rapidly increases. Thus, the incorporation of clay particles in chemically crosslinked PAAm hydrogels improves their mechanical properties. This improvement mainly appears above 4 % Laponite concentrations. The action of Laponite as a crosslinker is due to strong interactions at the clay-polymer interface and the combination of polymer and inorganic components within a single material on a nanoscale level.

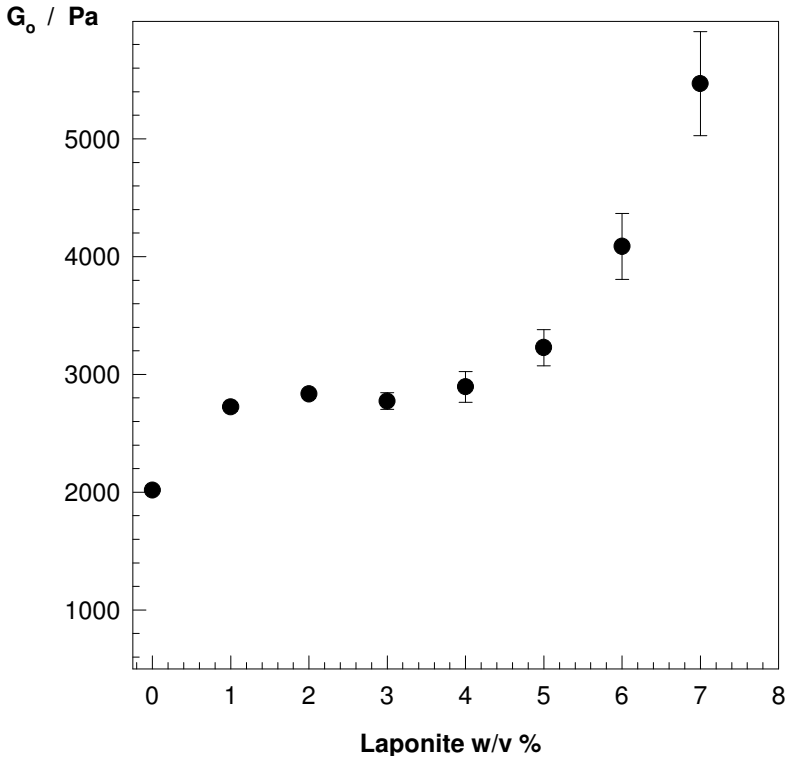

Figure 6.2 : The elastic modulus G_o of nanocomposite PAAm hydrogels just after their preparation shown as a function of the Laponite content in the reaction mixture.

We assume that the mechanism suggested by Haraguchi is also applicable to the formation of the present polymer-clay system containing the chemical crosslinker BAAm [10]. According to this mechanism, the monomers are first bound to the surface of the clay particles. This is due to the formation of hydrogen bonds between the oxygen atoms of clay and the amide protons of the monomers as well as due to the complex formation between the metal ions on the clay surface and the carbonyl oxygen

of the monomer. The decrease of the viscosity of clay dispersions with the addition of the monomer, as reported by Haraguchi [47], also suggests that the monomers effectively surround the clay particles. Since the monomer AAm is more hydrophilic than the crosslinker BAAm, the crosslinker ratio on the clay surface is expected to be lower than in the solution. Further, the initiator is also adsorbed on the clay surface by ionic interaction [7]. After decomposition of the initiator and, after formation of primary radicals, the polymer chains start to grow mainly from the surface of the particles until they terminate by recombination with other polymeric radicals bound by their other end to the surface of the clay particles. This type of termination results in the bridging of the particles and in the formation of effective network chains, while termination with un-anchored radicals or termination by disproportionation leads to the dangling chains. During the propagation step, the growing radicals also react with the crosslinker BAAm leading to the formation of pendant vinyl groups. The reactions of these pendant vinyl groups with radical centers lead to the formation of effective chemical crosslinks as well as of cycles and clusters of BAAm, as typical in crosslinking copolymerization of AAm and BAAm [46,52]. However, as seen in Figure 6.2, above 5 % Laponite, the elastic modulus of the hydrogels is mainly determined by the amount of clay. Thus, the network chains between the clay particles rather than those between the BAAm molecules determine the rubber elasticity of the nanocomposite hydrogels.

For the swelling measurements, the nanocomposite hydrogels with various amounts of Laponite were immersed in water for at least 3 months by replacing water every other day. It should be noted that, during the swelling experiments, Laponite particles inside the gel network may be extracted by water due to the fact that the polymer- particle interactions are physical in origin. In order to find out whether the particles remain inside the gel after the swelling process, equilibrium swollen nanocomposite hydrogels were dried until constant mass. Assuming that AAm monomer converts completely into the crosslinked polymer, the Laponite concentration C^{b}_{clay} inside the gel after extraction was calculated as:

$$C^{b}_{clay} = 10^{2} \frac{\left(m_{dry} - m_0 \, C_{AAm}/100\right)}{m_0} \qquad (6.1)$$

where m_0 and m_{dry} are the weights of the gel sample after preparation and after drying, respectively, C_{AAm} is the initial concentration of AAm monomer (5 w/v %). Note that equation 1 normalizes the Laponite concentrations inside the gel with respect to the after preparation state. In Figure 6.3, Laponite concentration C^{b}_{clay} inside the gel is plotted against its concentration C_{clay} used in the preparation of the nanocomposite hydrogels. If C^{b}_{clay} = C_{clay}, all the particles remain inside the gel network, indicating that the particles are bound strongly to the polymer chains. This condition is represented in the figure by the diagonal dotted line. Moreover, smaller values of C^{b}_{clay} indicate dissolution of the Laponite particles during swelling. It is seen that most of the Laponite used in the gel preparation remains inside the gel as bounded to the polymer chain.

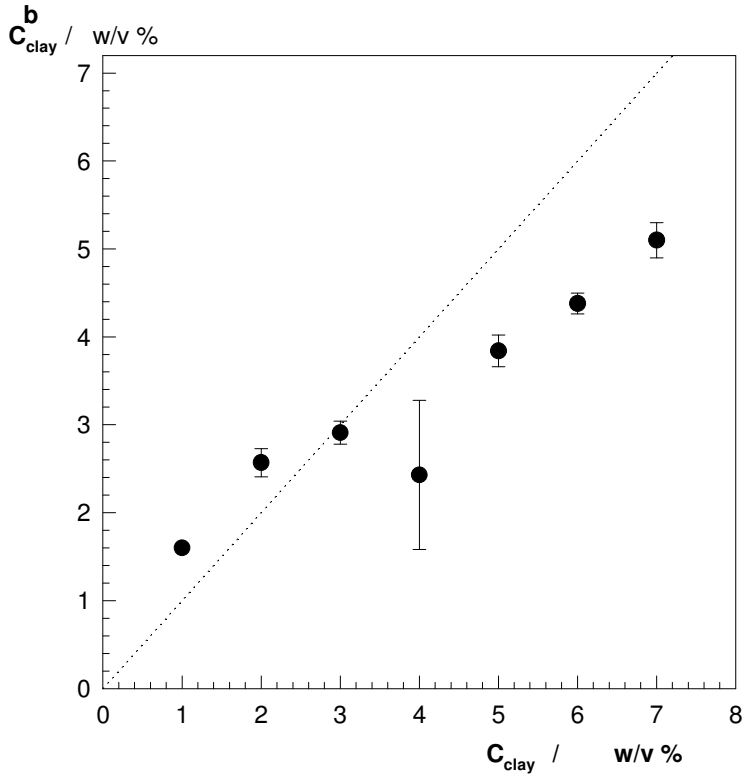

Figure 6.3: Laponite concentration C^{b}_{clay} used in the preparation of nanocomposite hydrogels shown as a function of its concentration Cclay in the reaction mixture

After the hydrogels attain their equilibrium state in water, their swelling capacities were measured. The results are shown in Figure 6.4, where the volume swelling ratio V/V_o is plotted against the Laponite concentration. The swelling ratio first decreases rapidly with the addition of Laponite but then, within the limits of the experimental error, it remains almost constant around 1.2.

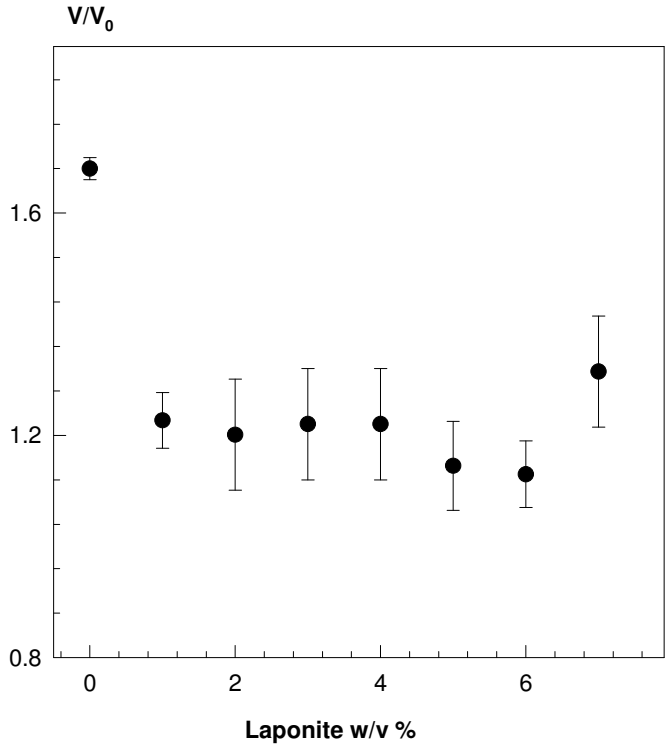

Figure 6.4: The equilibrium volume swelling ratio V/Vo of nanocomposite PAAm hydrogels shown as a function of the Laponite content in the reaction mixture.

The results shown in Figure 6.4 are rather unexpected since Laponite as a crosslinker should affect the swelling capacity of the hydrogels, especially in the concentration range between 4 and 7 %, where the elastic modulus rapidly increases (Figure 6.2). To understand the origin of this behavior, both the swelling and elasticity measurements were carried out as a function of the swelling time of the hydrogels in water. For this purpose, the nanocomposite hydrogels just after their preparation were immersed into water and, at certain time intervals, their swelling ratios V/V_o as well as their moduli of

elasticity G were measured. In Figures 6.5 and 6.6, the volume swelling ratio V/V_o and the elastic modulus G of the hydrogels are shown as a function of the swelling time, respectively. Laponite concentrations used in the hydrogel preparation are indicated in the figures. Several interesting features can be seen from the figures. At a Laponite concentration below 4 %, the swelling ratio increases while the elastic modulus slightly decreases with increasing time of swelling. After about 2 days, both V/V_o and G attain constant values indicating that the gels are in thermodynamic equilibrium with the solvent. Thus, the behavior of the nanocomposite hydrogels with less than 4 % Laponite is similar to the chemically crosslinked gels. However, at or above 4 % Laponite, the hydrogels first swell rapidly until a maximum degree of swelling is reached. During this period, the modulus of the hydrogels decreases and reaches a minimum value at the same time. At longer swelling times, the gels start to deswell again so that their swelling ratio decreases and modulus increases until attaining the equilibrium state in water after about one week.

This unusual self-deswelling behavior of the hydrogels with Laponite contents at or above 5 % has not been reported before. This behavior was also not observed in chemically crosslinked hydrogels and needs some explanations and comments. The time-dependent swelling and elasticity measurements mentioned above were conducted using gel samples taken out of the swelling solvent in certain time intervals. Thus, during the course of the swelling process, each gel sample was subjected to several elasticity (compression) tests. The pressure applied to the nanocomposite hydrogel samples during their swelling may be responsible for this behavior.

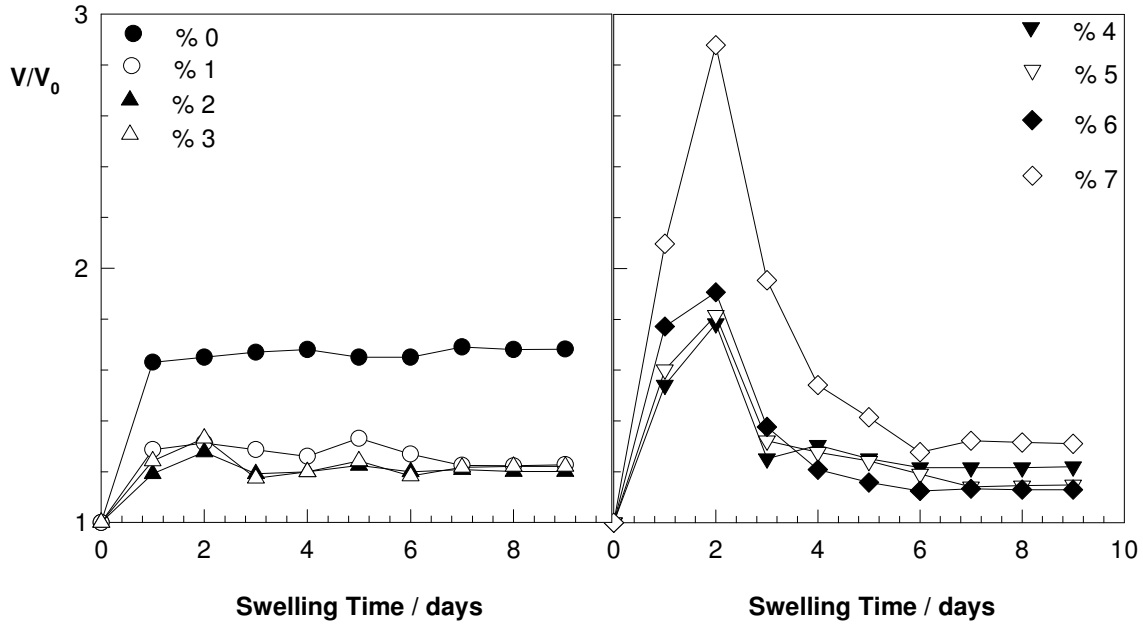

Figure 6.5: Volume swelling ratio V/Vo of the nanocomposite hydrogels shown as a function of the swelling time in water. Laponite contents are indicated in the figures.

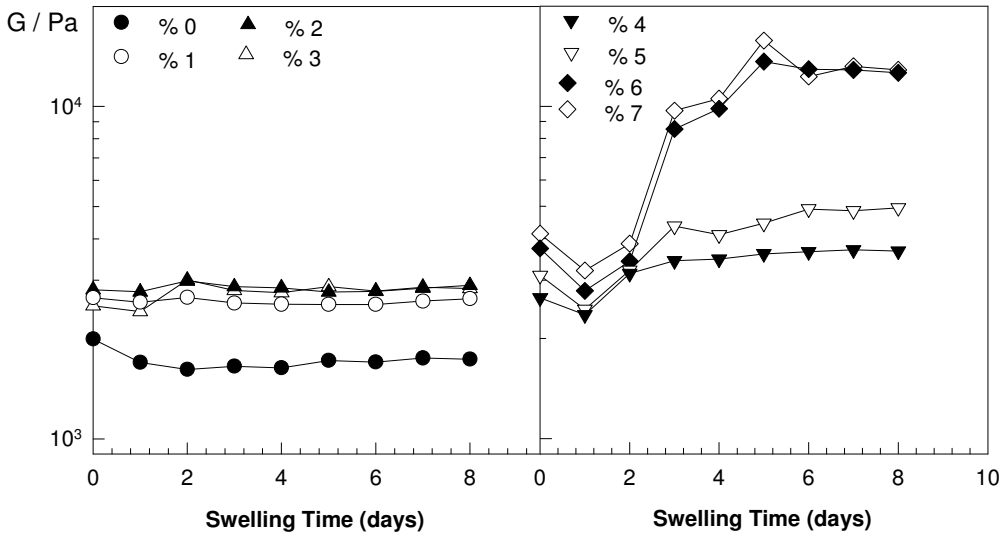

Figure 6.6: The elastic modulus G of the nanocomposite hydrogels shown as a function of the swelling time in water. Laponite contents are indicated in the figures.

To check whether the unusual swelling and elasticity behavior of the hydrogels is due to the pressure applied during the elasticity tests, experiments with hydrogels containing 7 % Laponite were repeated using single and multiple measurements. In the single measurements, several hydrogel samples were immersed separately into water and the gel samples were taken out of the solvent one by one at certain times for the measurements. Thus, the nanocomposite gels were not perturbed during their swelling process. The multiple measurements were conducted by use of a single gel sample, as before. Here, the same gel sample was subjected several times to the elasticity tests during its swelling. The results of the swelling and elasticity tests are shown in Figure 6.7. Here, the volume swelling ratio V/V_o and the elastic modulus G of the hydrogels are shown as a function of the swelling time, respectively. The results of single and multiple measurements are shown in the figure by the filled and open symbols, respectively. As shown in the figure, both of the measurement techniques gave similar tendency in the time-dependence of the swelling ratio and the modulus of the elasticity of the hydrogels. The result clearly indicates that the observed behavior does not originate from the method of measurements and thus, it is real and originates from the variation of the gel crosslink density during the course of the gel swelling.

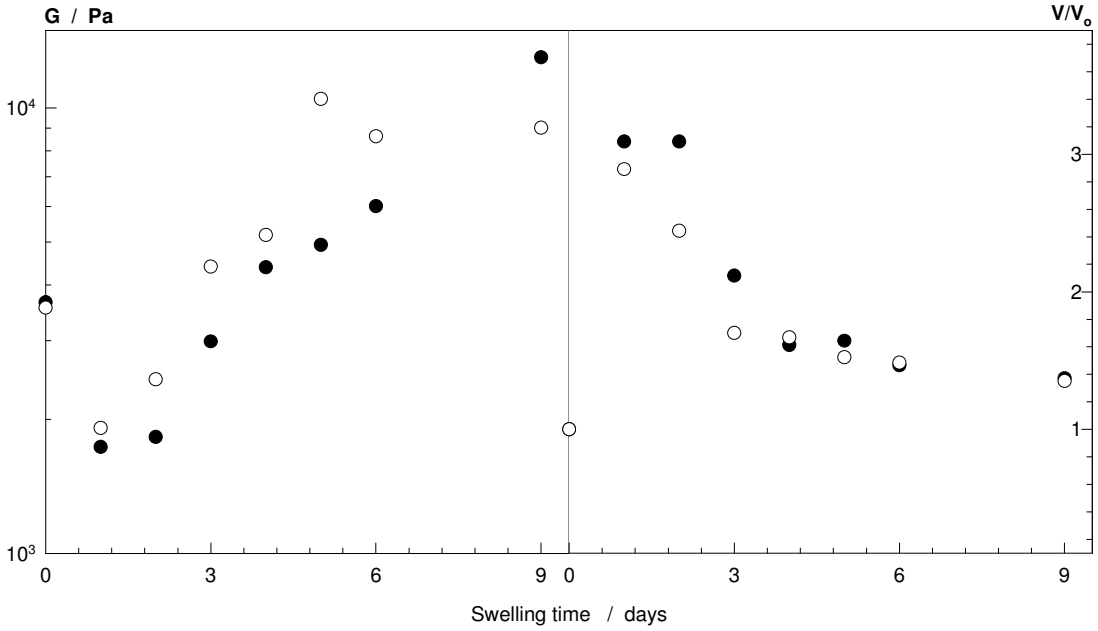

Figure 6.7: Variation of the volume swelling ratio V/Vo and the elastic modulus G of the nanocomposite hydrogels as a function of the swelling time in water. Filled and

open symbols represent the results of single und multiple measurements. Laponite content = 7 w/v %.

The crosslink density ν_e of the nanocomposite hydrogels was calculated from their elastic modulus *G* together with the equation [16, 20]:

$$G = A\,\nu_e\,RT\,(\nu_2)^{1/3}\left(\nu_2^0\right)^{2/3} \qquad (6.2)$$

where the front factor A equals to 1 for an affine network and 1- 2 / ϕ for a phantom network, ϕ is the functionality of the crosslinks, ν_2^0 and ν_2 are the volume fractions of crosslinked polymer in the gel just after preparation and at the state of the measurements, respectively, *R* is the gas constant and *T* is the temperature. Assuming complete conversion of the monomer AAm to the crosslinked polymer and since the density of PAAm is 1.35 g/cm^3, ν_2^0 was calculated as 0.037 for all the hydrogels. Further, ν_2 relates to ν_2^0 by the equation:

$$\nu_2 = \frac{\nu_2^0}{V/V_0} \qquad (6.3)$$

Using equations 2 and 3, and assuming affine network behavior, the effective crosslink densities of the nanocomposite hydrogels were calculated for various Laponite contents and swelling times. The results are shown in Figure 6.8 plotted against the swelling time.

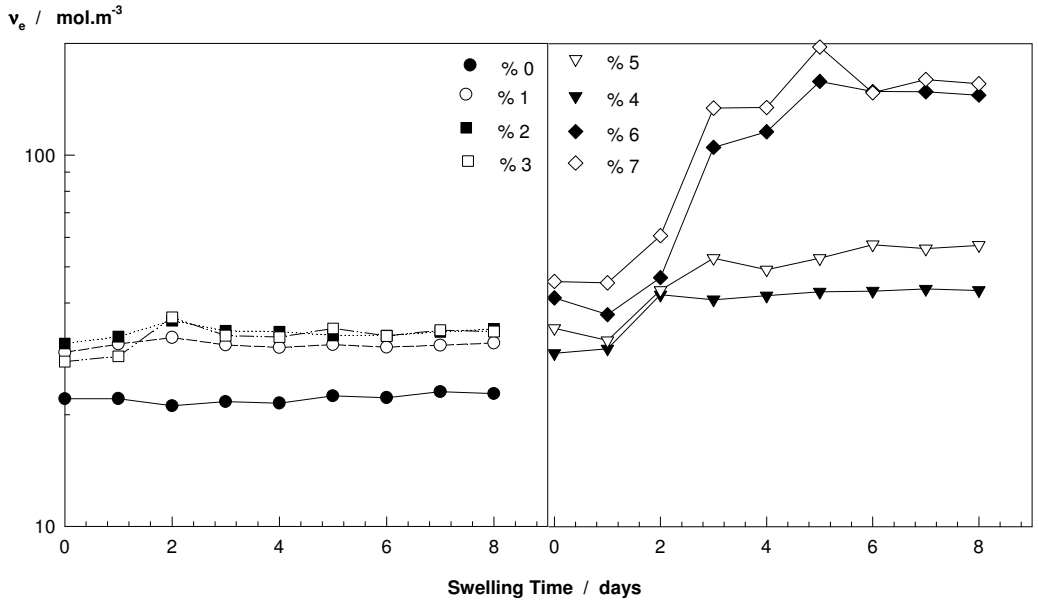

Figure 6.8: Variation of the effective crosslink density ν_e of the nanocomposite hydrogels with the swelling time. The Laponite contents are indicated in the figure.

As shown in the figure, the effective crosslink density ν_e of the hydrogels with less than 4 % Laponite remains constant during the course of swelling. This is a general behavior observed in chemically crosslinked hydrogels. However, the crosslink density of the hydrogels with 4 % Laponite or above increases with the time of swelling and this increase is drastic at high Laponite contents. For example, equilibrium swollen nanocomposite hydrogels with 6 – 7 % Laponite exhibit crosslink densities which are more than three-fold larger than those of the hydrogels just after their preparation. This results thus obtained indicate that some additional crosslinks form inside the gel network during the course of the swelling process. These "post crosslinking reactions" may be explained according to the following scenario:

1- The gel first swells in water due to the fact that water is a good solvent for PAAm chains. As the gel swells, the network chains assume a more elongated conformation so that the probability that the chain segments interact with the Laponite particles increases.

2- Laponite stacks, as schematically shown in Figure 6.1A, that did not exfoliate properly during the preparation of the reaction solutions, is exfoliated during the swelling process. This is due to the increasing volume of gel, which decreases the Laponite concentration in the gel solution.

3- The newly exfoliated clay particles together with the particles that formed ineffective crosslinks after the state of gel preparation attach on the network chains and leads to the formation of additional Laponite bridges, i.e., additional crosslinks.

Figure 6.9 shows the stress – strain data of the nanocomposite hydrogel with 7 % Laponite at various swelling times. It is seen that the stress – strain dependence of the gel, which is linear at short swelling times, start to bend after one day. A significant bending of the curves was observed at long swelling times. From the shape of the curves, one may distinguish two different slopes, namely one at low pressure side and the other at high pressure side. While the slope at low pressures, that is, the modulus G of the hydrogel increases with the swelling time, the slope at high pressures decreases and approaches to the value of the modulus G_o of the gel just after preparation.

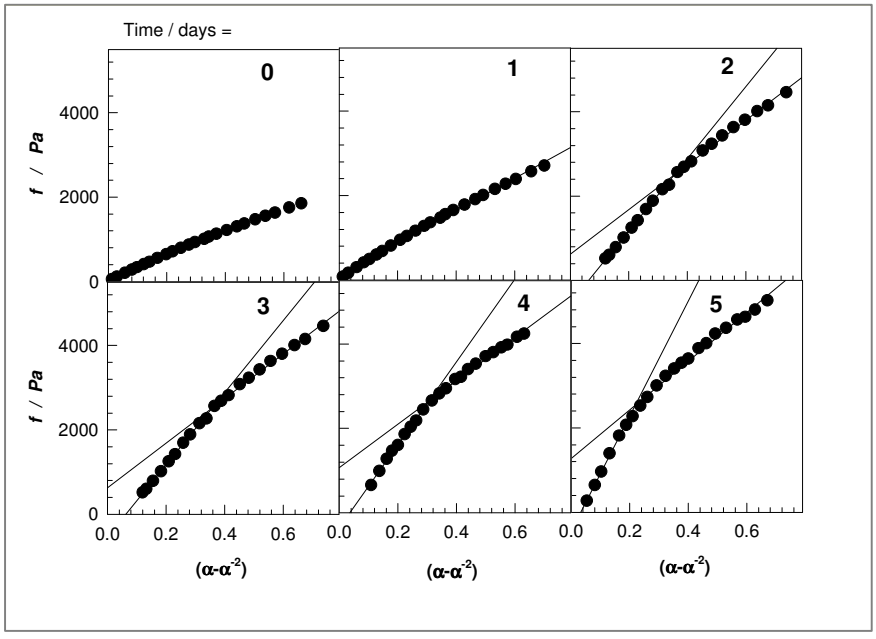

Figure 6.9: Stress – strain curves of the nanocomposite hydrogel with 7 % Laponite obtained at various swelling times indicated in the figures.

Similar results were also observed using hydrogels containing 6 % Laponite, as shown in Figure 6.10. Here, the bending of the stress-strain curves start to appear after a swelling time of 5 days.

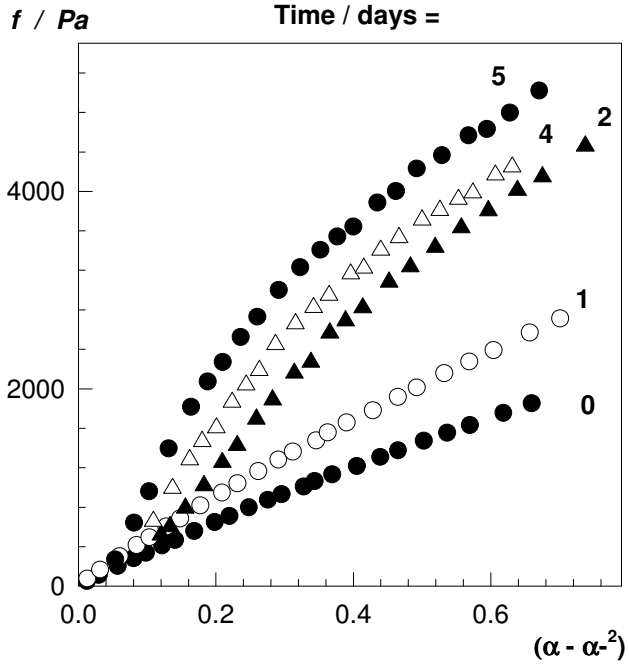

Figure 6.10: Stress – strain curves of the nanocomposite hydrogel with 6 % Laponite obtained at various swelling times indicated in the figures.

In Figure 6.11, the stress-strain dependences of the nanocomposite hydrogels containing varying amounts of Laponite are given. The swelling time was fixed at 7 days. It is seen that the hydrogels with a low amount of Laponite show a linear variation of strain with the applied stress. Deviation from the linearity mainly appears at high Laponite contents suggesting that the bending of the curves is related with the Laponite particles. The behavior can be explained with the post crosslinking reactions occurring inside the gel. Since PAAm chains are bounded physically by the Laponite particles, desorption occurs at high pressures so that the elastic modulus returns to its initial value of G_0. This desorption mainly occurs at high Laponite contents, probably due to the presence of weak, additional crosslinks formed by post-crosslinking reactions, which can be broken down under the mechanical force.

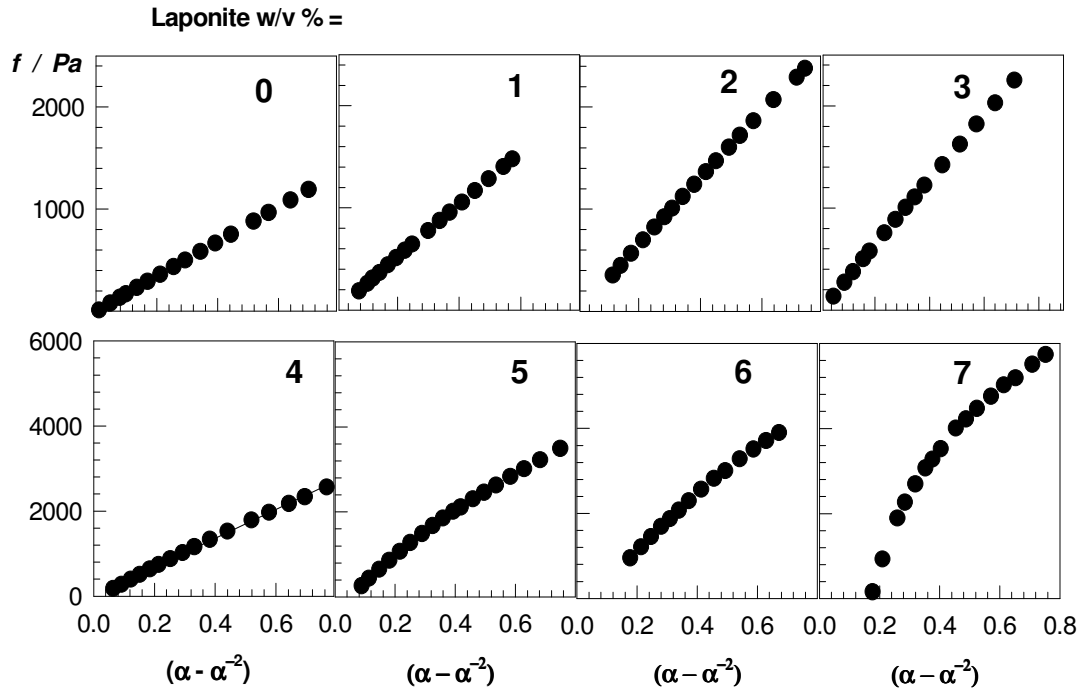

Figure 6.11: Stress – strain curves of the nanocomposite hydrogels with various Laponite contents indicated in the figures. Swelling time = 7 days

The stress – strain experiments were also carried out up to very large compression ratios of gels. Typical results of such measurements are shown in Figure 6.12. Here, an equilibrium swollen nanocomposite hydrogel sample with 7 % Laponite was compressed up to 80 % of its initial length. Despite 80 % compression, the gel doesn't crash while the modulus decreases to about 1/3 of the initial value.

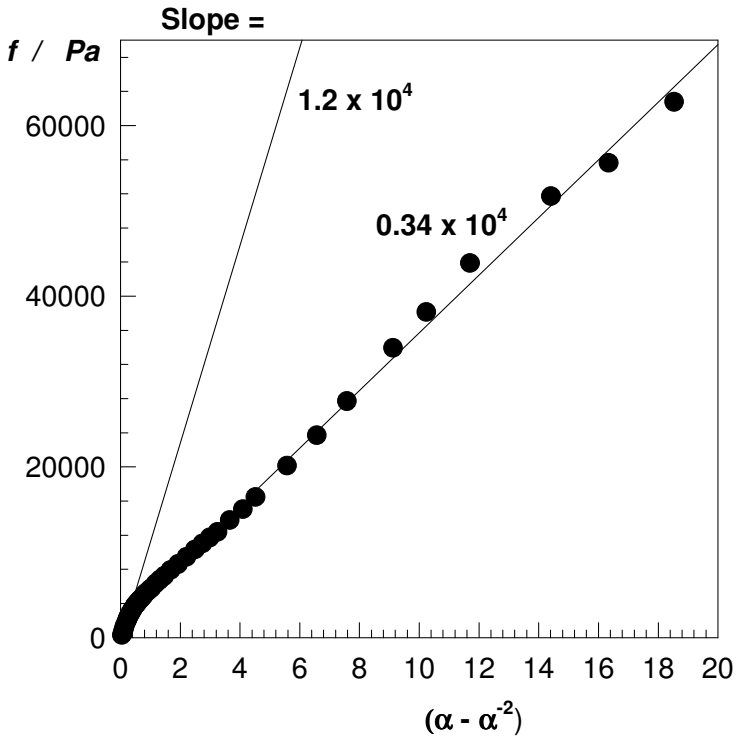

Figure 6.12: Stress – strain curve of a swollen nanocomposite hydrogel up to 80 % compression. Laponite content = 7 %.

6.3. Effect of BAAm concentration on the properties of nanocomposite hydrogels

In the second set of experiments, the crosslinker ratio *X*, that is the molar ratio of the chemical crosslinker BAAm to the monomer AAm was changed between 1/80 and 1/1000 while the Laponite concentration was fixed at 7 w/v %. As in the previous section, the variations of both the elastic modulus and the swelling ratio of the gels were investigated as a function of the crosslinker ratio and the time of swelling.

Figure 6.13 shows the volume swelling ratio V/Vo and the elastic modulus G of the nanocomposite hydrogels as a function of the swelling time in water. The chemical crosslinker ratios X used in the hydrogel preparation are indicated in the figure. It is seen that all the hydrogel samples exhibit the unusual swelling behavior reported in the previous section. They first swell until achieving a maximum gel volume but then they deswell again until the equilibrium state is reached after about one week. During this

process, the modulus of elasticity first decreases and after passing a minimum, it increases again until a limiting value is obtained. Comparison of the behavior of gels formed at different crosslinker ratios shows that the lower the chemical crosslinker ratio, the larger is the extent of the variations of both the gel volume and the elastic modulus.

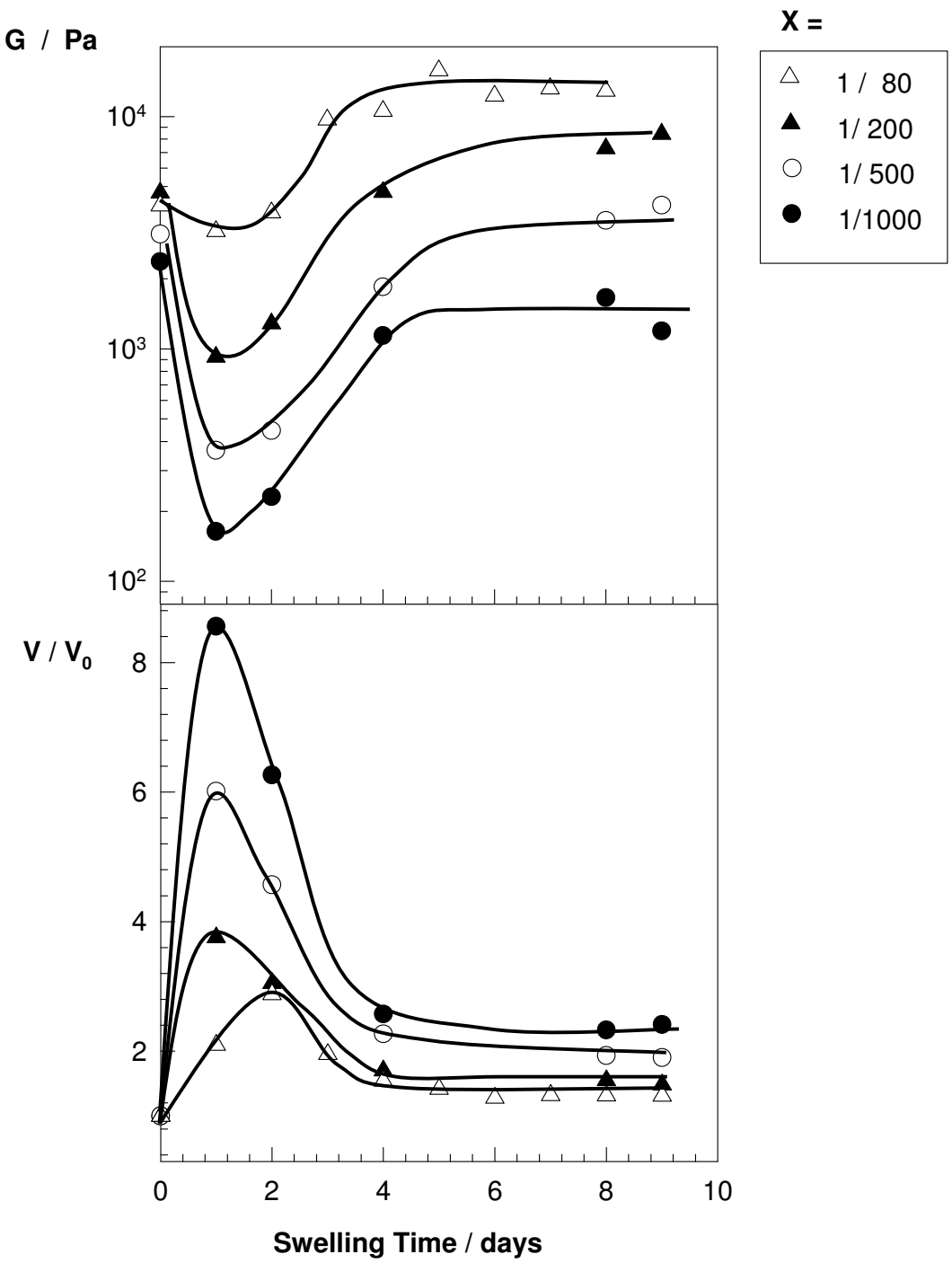

Figure 6.13: Variations of the volume swelling ratio V/Vo and the elastic modulus G of the nanocomposite hydrogels as a function of the swelling time in water. The chemical crosslinker ratios X used in the hydrogel preparation are indicated in the figure. Laponite content = 7 w/v %.

The results shown in Figure 6.13 were obtained by taking the gel samples out of the swelling agent at certain time intervals. We also monitored the swelling process of the nanocomposite hydrogels in situ using an optical microscope connected to a PC with the image analyzing system Image Pro Plus. Thus, in these experiments, the gel samples were in continuous contact with water. The diameter of the gel samples was recorded automatically as a function of time. The results are shown in Figure 6.14 where the volume swelling ratios V/Vo are plotted against the swelling time in water.

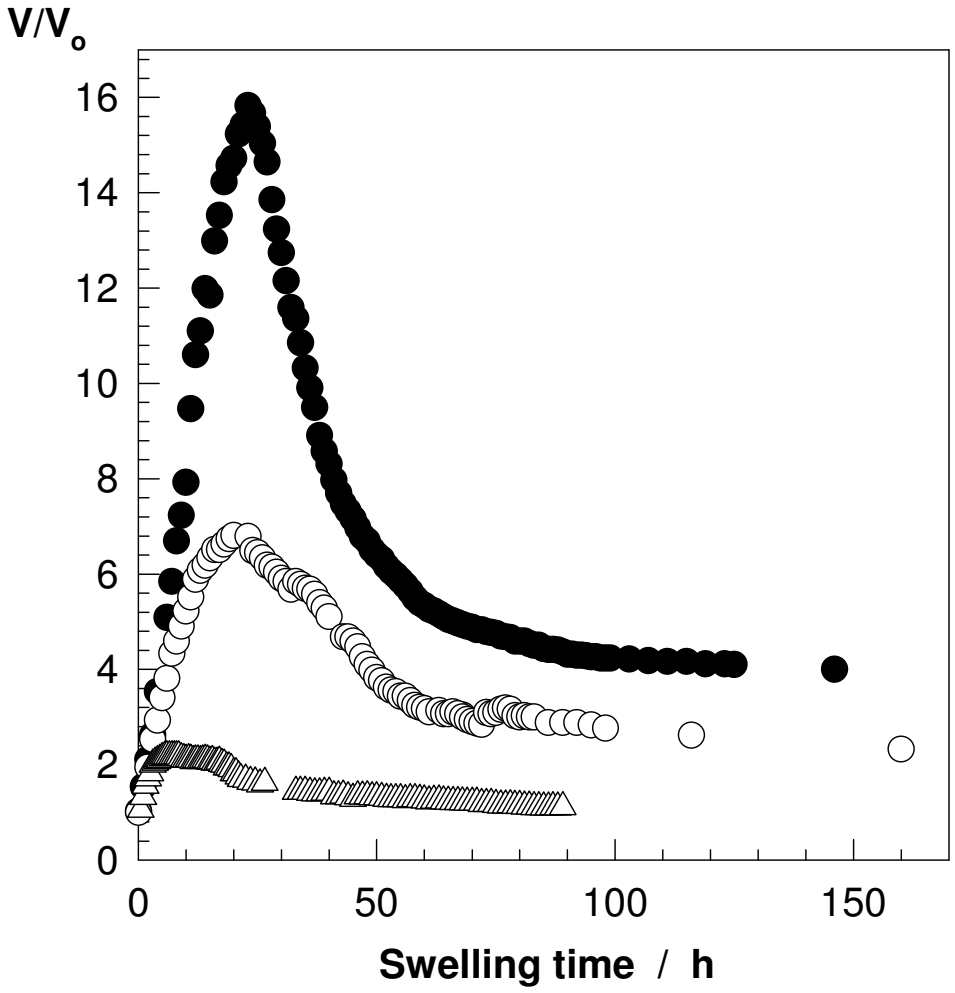

Figure 6.14: On-line monitoring of the nanocomposite gel volume as a function of the swelling time. The volume swelling ratio V/Vo is shown as a function of the swelling time for hydrogels with a crosslinker ratio 1/1000 (●), 1/500 (○) and 1/80 (△). Laponite contents are 7 w/v.

Comparison of Figures 6.13 and 6.14 shows that, although the swelling profiles are the same, in-situ measurements lead to larger gel volumes compared to the batch measurements. This may be related to the increasing extent of extraction of Laponite particles in the batch technique.

6.4. Effect of salt concentration on the swelling properties of nanocomposite hydrogels

As mentioned before, Laponite clay has a structural negative charge which is neutralized by the Na^+ ions absorbed onto the surfaces of the particles. Thus, Laponite may be expected to act both as a crosslinker and as an ionic component in the formation of nanocomposite hydrogels. To demonstrate the ionic character of the nanocomposite hydrogels, we investigated their swelling behavior in aqueous NaCl solutions. As is well known, ionic hydrogels deswell as the salt concentration in the external solution is increased while the volume of non-ionic gels remain unchanged [50].

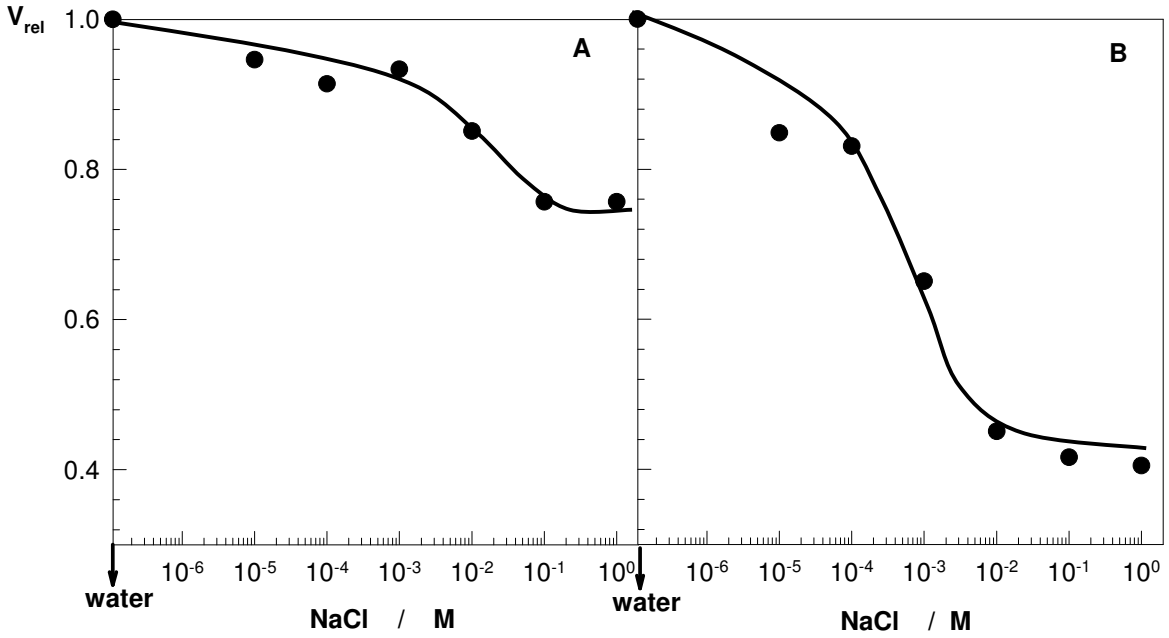

Figure 6.15: Relative volume swelling ratio V_{rel} of the nanocomposite hydrogels with 7 % Laponite shown as a function of NaCl concentration. The crosslinker ratio X = 1/80 (A) and 1/1000 (B). The solid curves are guide to the eye.

In Figure 6.15A and 6.15B, the relative volume swelling ratios V_{rel} (equilibrium gel volume in salt solution / gel volume in water) of the hydrogels with a crosslinker ratio of 1/80 and 1/1000, respectively, are shown as a function of the salt concentration. The Laponite contents of the hydrogels were 7 w/v %. Deswelling of the hydrogel with increasing salt concentration in the external solution is seen from the Figure. This deswelling is significant for the hydrogels with a lower crosslinker ratio. The deswelling of gels with the salt concentration reveals the ionic character of the nanocomposite hydrogels. Thus, hydrogels, when immersed in water, Na^+ counterions absorbed on the Laponite particles inside the gel creates an osmotic pressure. This is due to the concentration difference of the counterions between the inside and outside the gel phase. As a consequence, the hydrogel swells much more than the corresponding hypothetical nanocomposite hydrogel without mobile ions. As the salt concentration in the external solution is increased, the concentration difference of counterions inside and

outside the hydrogel decreases, which induces deswelling of the hydrogels. According to Figure 6.15, at a salt concentration of 10^{-1} M or above, all the charged groups inside the hydrogels are screened so that they behave as non-ionic hydrogels. The answer of the question why the hydrogels with a higher crosslinker ratio deswells in salt solution much lesser amount than those with a lower crosslinker ratio is unclear.

6.5 Effect of acetone on the extent of polymer – clay interactions

By the preliminary experiments, we observed that the nanocomposite hydrogels prepared without the chemical crosslinker BAAm dissolves in aqueous solutions of acetone at certain acetone contents. This behavior is seen in Figure 6.16, where the relative weight swelling ratio m_{rel} (mass of gel in the solution / mass of gel in water) is plotted against the acetone content of acetone-water mixtures. The gel collapses in acetone solutions containing more than 50 % acetone by volume. This is due to the fact that acetone is a poor solvent for PAAm chains so that the network chains shrink in these solutions. However, in solutions containing between 20 and 40 % acetone, the gel gradually dissolves indicating that the Laponite bridges between the PAAm chains become instable in these solutions.

Based on the above findings, we designed the following strategy to affect the properties of the nanocomposite hydrogels using the treatment with acetone. As seen in Figure 6.3, the equilibrium swollen hydrogel with a chemical crosslinker ratio X = 1/80 exhibits an elastic modulus of about 13 kPa and 1.7 kPa for Laponite contents of 0 and 7 %, respectively. Thus, Laponite induces a 8-fold increase in the elastic modulus of the swollen gel. Conversely, extraction of the nanocomposite hydrogel with acetone solution would result in an 8-fold decrease in the elastic modulus of the hydrogel.

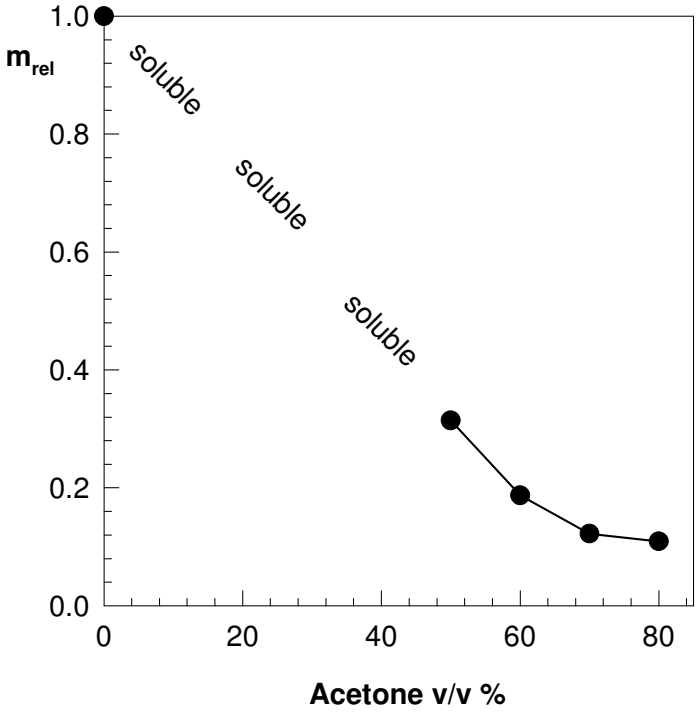

Figure 6.16: Relative weight swelling ratio m_{rel} of the nanocomposite hydrogels with 8 % Laponite shown as a function of acetone content of acetone-water mixtures. The crosslinker ratio X = 0.

In order to proof this idea, the swollen hydrogel samples with 7 % Laponite were first immersed in aqueous acetone solutions for one month replacing the solution every other day. Then, the extracted hydrogels were immersed into water and after attaining the equilibrium state; their moduli as well as their swelling ratios were measured. The results are collected in Figures 6.17. Here, the elastic modulus G and the volume swelling ratio V/V_o of the hydrogels in water are shown as a function of the acetone content of the solution used in the extraction. The data shown at 0 % acetone correspond to those of the original hydrogel sample without the extraction. As can seen from the figure, the gels immersed in 10 and 20 % acetone by volume show a lower modulus and a higher swelling ratio compared to the original hydrogel. This means that, not all, but a part of the Laponite particles inside the gel could be removed by this extraction. This also demonstrates that Laponite is physically bonded to PAAm chains

inside the gel network. Figure 6.17 also shows that, at higher acetone concentrations, the moduli increase and the swelling ratio decreases. This behavior can be explained as follows: The nanocomposite hydrogel immersed into acetone solution deswells so rapid that Laponite can not escape outside the gel phase. Since the clay particles and polymer chains can interact more easily in a smaller gel volume, the number of contact between Laponite and polymer increases. Hence, when the gel re-swelled back in pure water, these interactions remain intact so that the hydrogel exhibits a higher modulus and lower swelling degree compared to the original hydrogel.

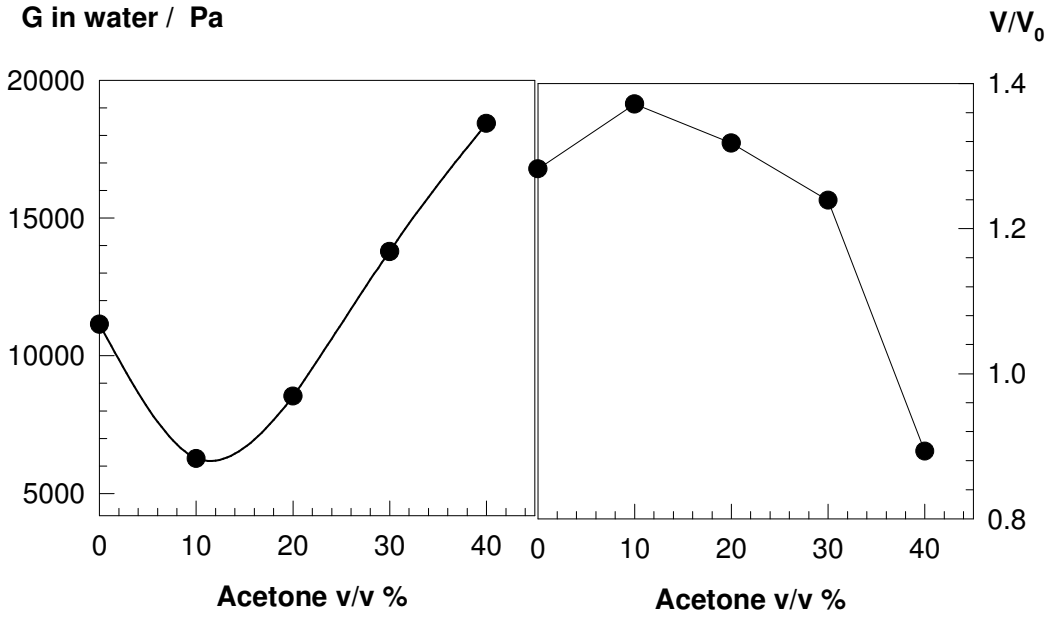

Figure 6.17: Elastic modulus G and the volume swelling ratio V/V_0 of the nanocomposite hydrogels with 7 % Laponite shown as a function of acetone content of acetone-water mixtures used in the extraction. The crosslinker ratio X = 1/80.

6.6. Effect of poly(ethylene oxide) on the properties of nanocomposite hydrogels

As is well known, addition of water-soluble polymers affects the properties of Laponite dispersions. It was shown that the binding between the particles can be inhibited by adding low molecular weight poly(ethylene oxide) (PEO) due to the saturation of the

particles with an adsorbed layer of polymer chains [12,51,52]. Higher molecular weight PEO bridges between the particles leads to the formation of clusters or a weak gel immediately after mixing [53]. Thus, polymers that are long enough to form interparticle bridges will promote formation of a reversible clay-polymer network. Moreover, depending on the surface coverage of the Laponite particles by the polymer chains, Laponite-PEO mixtures exhibit physical properties ranging from a low viscosity liquid up to an elastic gel [52]. Zebrowski et al. and Can et al. showed that, for certain concentrations of Laponite and PEO as well as in a certain molecular weight range of PEO, Laponite – PEO mixtures undergo shear-induced gelation and the gels formed transform again into a liquid if the shear stops [53, 54]. Such gels are called as "shake gels".

In order to find out the effect of PEO addition on the properties of the nanocomposite hydrogels, the hydrogels with a crosslinker ratio X = 1/80 were immersed in aqueous solutions of PEO of molecular weight 10000 g/mol. Figure 6.18 shows the variation of the elastic modulus and the volume swelling ratio of the hydrogels equilibrium swollen in PEO solutions plotted against the PEO concentration in the external solution. Filled symbols are for the hydrogels with 7 % Laponite while the open symbols are for those without Laponite. Using the experimental data shown in Figure 6.18 together with equations 2 and 3, we also calculated the effective crosslink densities ν_e of the hydrogels. The results are shown in Figure 6.19 plotted against the PEO concentration for the hydrogels with (filled symbols) and without Laponite (open symbols).

It is seen that, the conventional hydrogel (without Laponite) deswells continuously as the PEO concentration is increased, while its crosslink density remains unchanged. This is expected due to the following reasons:

a) The size of the PEO coils of molecular weight 10000 g/mol is relatively large for the mesh size of the gel network, so that a significant fraction of the linear chains remains in the external solution. Thus, the concentration difference of PEO between the inside and outside the gel creates an osmotic pressure so that the gel deswells with increasing PEO

concentration. This deswelling is continuous since the higher the PEO concentration, the higher the osmotic pressure compressing the hydrogel.

b) Since the chemical crosslinks formed due to the BAAm molecules are stable in the conventional hydrogel, its crosslink density does not change with the PEO concentration. Although the entanglements between PEO chains penetrating into the gel and PAAm network chains may form additional crosslinks, this effect seems to be negligible.

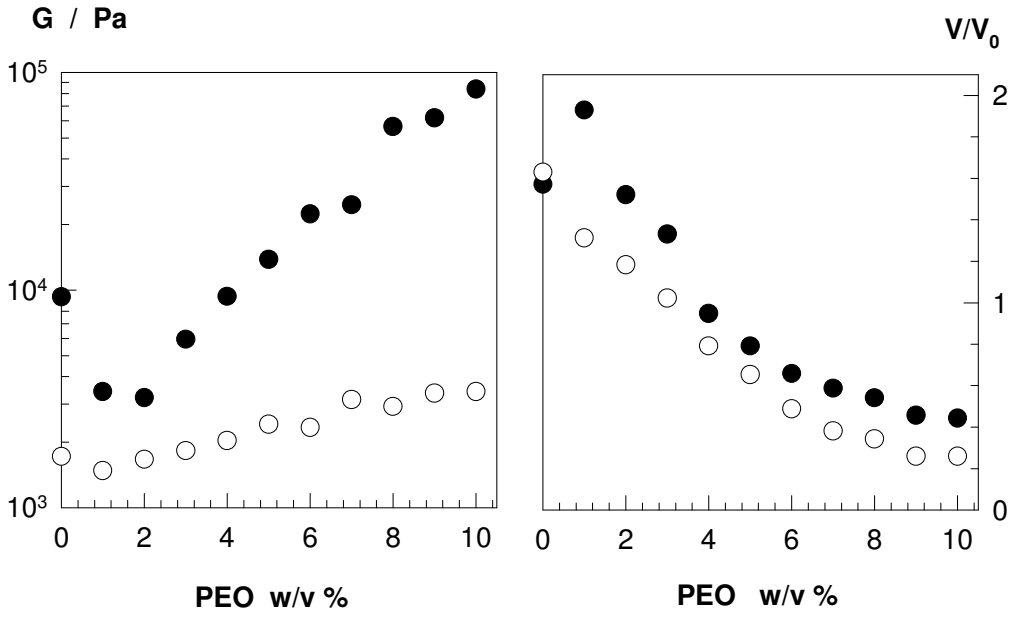

Figure 6.18: Variation of the elastic modulus G and the volume swelling ratio V/Vo of the nanocomposite hydrogels immersed in aqueous solutions of PEO -10000 as a function of PEO concentration. Laponite = 0 (○) and 7 % (●).

In contrast to the conventional hydrogel, the nanocomposite hydrogel immersed in PEO solution first swells up to 1 % PEO but then continuously reswells as the PEO

concentration is increased. Moreover, Figure 6.19 demonstrates that the swelling and deswelling of the gel are accompanied with the variation of its effective crosslink density. At PEO contents up to 2 %, the crosslink density decreases and it approaches to the value of the conventional hydrogel. This indicates that the PEO chains entering in the gel phase cover the particles due to the strong PEO-clay interactions, so that the particles with an adsorbed layer of PEO chains lost their bridging ability between PAAm chains.

However, at higher PEO contents, the crosslink density increases abruptly up to about one order of magnitude larger value compared to the initial crosslink density measured in water. The significant increase in the crosslink density suggests formation of additional crosslinks in the nanocomposite hydrogel. One may speculate that PEO forms interparticle bridges between the particles so that the particles forming ineffective crosslinks are converted into elastically effective junction points.

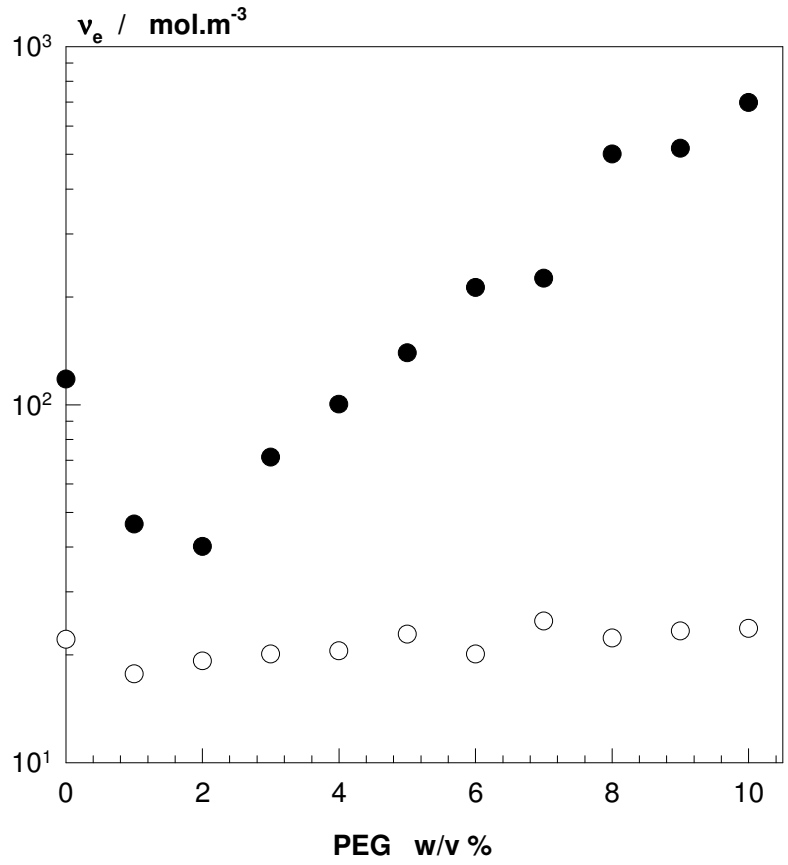

Figure 6.19: Variation of the crosslink densities ν_e of the nanocomposite hydrogels (X = 1/80) as a function of PEO – 10000 concentration in the external solution. Laponite = 0 (○) and 7 % (●).

Hydrogels equilibrium swollen in PEO solutions were immersed back into pure water and, after attaining the new swelling equilibrium state, their swelling ratios and elastic moduli were measured. The results are shown in Figure 6.20 where the elastic modulus G and the volume swelling ratio V/Vo of the equilibrium swollen nanocomposite hydrogels (filled symbols) and conventional hydrogels (with no Laponite, open symbols) are shown as a function of the PEO content of solutions from which they were taken out before immersing into water. The hydrogels taken out of PEO solutions exhibit a lower moduli of elasticity similar to the conventional hydrogel (open symbols). However their volume swelling ratios are about twice of the latter hydrogels.

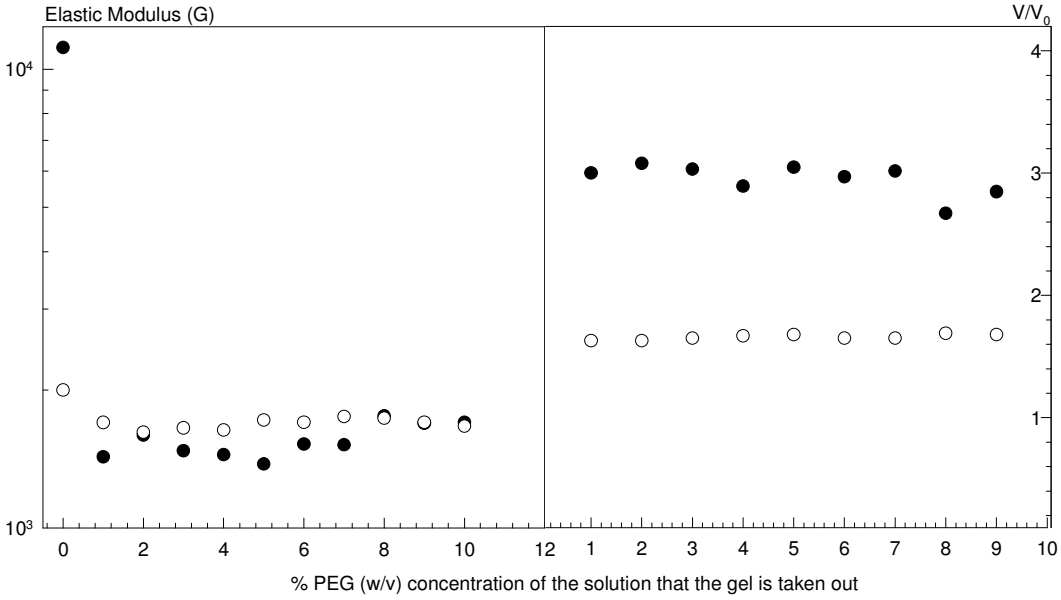

Figure 6.20: Variation of elastic modulus G and the volume swelling ratio V/Vo of the equilibrium swollen nanocomposite hydrogels (filled symbols) and conventional hydrogels with no Laponite (open symbols) shown as a function of the PEO content of solutions from which they were taken out before immersing into water.

This swelling behavior can be explained with the hydrolysis of PAAm network chains. It is known that the AAm segments in hydrogels gradually hydrolyze to acrylic acid under basic conditions [55]. Since pH of Laponite, when dissolved in water is 10 [34], the gel solution is basic so that the hydrolysis can proceed with increasing time of swelling. As a consequence, the swelling capacity of gels increases. Increasing degree of swelling necessarily decreases the concentration of the network chains so that the modulus increases.

6.7. Preparation of nanocomposite hydrogels in PEG solutions:

In this section, we prepared the nanocomposite hydrogels in aqueous PEO solutions instead of water. The chemical crosslinker ratio X and the Laponite concentration were fixed at 1/80 and 7 %, respectively. The use of PEO solution instead of water as the

polymerization solvent would produce hydrogels with better mechanical properties. This is due to the fact that, in addition of PAAm chains, PEO chains will also interact with the Laponite particles so that the effective crosslink densities will increase compared to the un-modified nanocomposite hydrogels. In Figure 6.21, the volume swelling ratio V/Vo and the elastic modulus G of the nanocomposite hydrogels are shown as a function of the swelling time in water. Hydrogels were prepared in PEO solutions at various PEO contents as indicated in the figure. As discussed in the previous sections, the hydrogels modified with PEO chains first deswell but then re-swell again with increasing time of swelling. This swelling process is accompanied with an initial decrease followed by a rapid increase in the modulus of the hydrogels. Figure 21 also shows that, in contrast to the expectation that the mechanical properties of the hydrogels will improve further, no substantial change in the properties was observed.

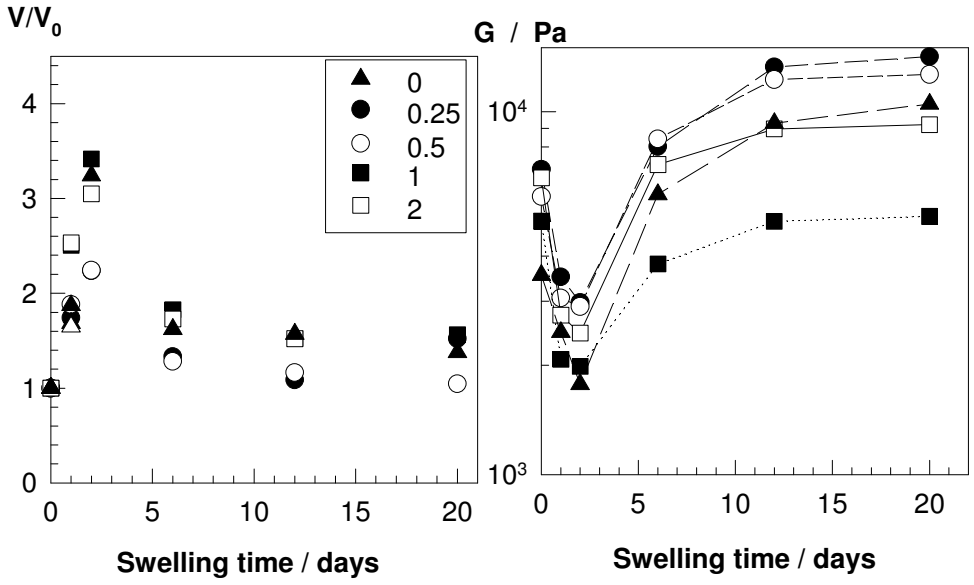

Figure 6.21: Variation of the volume swelling ratio V/Vo and the elastic modulus G of the nanocomposite hydrogels as a function of the swelling time in water. Hydrogels were prepared in PEO solutions of PEO contents (w/v %) indicated in the figure. Laponite = 7 %. X = 1/80.

7. CONCLUSION

The swelling behavior and the elastic properties of nanocomposite hydrogels have been investigated. The hydrogels were prepared by free-radical polymerization of the monomer acrylamide (AAm) in aqueous clay suspensions at 21^{o}C. Laponite XLS with a radius of 25 nm was used as clay particles in the hydrogel preparation. The reactions were carried out in the presence of the chemical crosslinker N, N'-methylenebis(acrylamide) (BAAm).

It was found that the nanocomposite hydrogels based on PAAm as the hydrophilic polymer component and Laponite XLS as the clay component exhibit unusual swelling behavior in water. They first rapidly swell and attain a maximum swelling ratio after about one day. Further increase in the swelling time results in the deswelling of the gels until they reach a limiting swelling ratio after about 5 days. This type of swelling behavior is observable only, when the clay concentration in the hydrogel is above a critical concentration. Swelling measurements combined with the elasticity tests show that the effective crosslink density, ν_e, of the hydrogels first decreases, but then increases with increasing time of swelling. The extent of the variations in ν_e becomes significant as the clay content is increased or, as the chemical crosslinker ratio *X* is decreased. The results were explained in terms of the rearrangements of the highly entangled polymer chains and clay particles during the course of swelling. It was also shown that the nanocomposite hydrogels become unstable and dissolve in dilute aqueous solutions of acetone or PEO of molecular weight 10000 g/mol.

8. REFERENCES

[1] **Tanaka, T**., *Gels, Sci.Am*., 1981, **244**,110-123

[2] **Y. Osada and K. Kajiwara**, "Gels Handbook'', Ed., Academic Press, Elsevier, Amsterdam, 2000.

[3] **Shibayama, M.**, *Macromol. Chem. Phys*., 1998. **199**, 1.

[4] **Tanaka Y, Gong JP, Osada Y**. *Prog Polym Sci* 2005;**30**:1

[5] **Okumura Y., Ito K**. *Adv. Mater.* 2001, **13**, 7, 485

[6] **Gong, J.P, Katsuyama Y., Kurukawa T., Osada, Y**. *Adv. Mater*. 2003, **15**, 14

[7] **Haraguchi K, Takehisa T**. *Adv Mater* 2002;**14**:1120

[8] **Haraguchi K, Takehisa T, Fan S.** *Macromolecules* 2002;**35**:10162

[9] **Haraguchi K, Farnworth R, Ohbayashi A, Takehisa T.** *Macromolecules* 2003;**36**:5732

[10] **Haraguchi K, Li HJ, Matsuda K, Takehisa T, Elliott E.** *Macromolecules* 2005;**38**:3482

[11] **Mongondry P, Tassin J-F, Nicolai T.** *J Colloid Interface Sci* 2005;**283**:397

[12] **Mongondry P, Nicolai T, Tassin J-F.** *J Colloid Interface Sci* 2004;**275**:191

[13] **Nie J, Du B, Oppermann W.** *Macromolecules* 2005;**38**:5729

[14] **Okay O, Oppermann W.** *Macromolecules* 2007;**40**:3378

[15] **Flory, P.J.**, *J. Chem, Phys.,* 1942. **10**, 51.

[16] **Flory, P.J.**, Principle of Polymer Chemistry, Cornell University Press, Ithaca, NewYork 1953

[17] **Huggins, M.L.**, *Ann. N.Y.Acad.Sci.,* 1942. **43**,1.

[18] **Young, R.J., Lovell, P.A.**, *Introduction To Polymers*, 1991. Chapter III, p.139,141,142.

[19] **Wall, F.T.**, *J. Chem. Phys.* 1942, **10**, 485

[20] **Treloar, L.R.G**:, The Physics of Rubber Elasticity, University Press, Oxford. 1975.

[21] **Flory, P.J. and Rehner, J.,** *J. Chem. Phys.,* 1943. **11**, 521.

[22] **James, H. M. and E. Guth.**, *J. Chem. Phys*. 1943. **11**, 455

[23] **J.P. Queslel and J.E. Mark**, Encyclopedia of Physical Science and Technology, 1987. **12**, 385.

[24] **Kuhn, W.**, *Kolloidszchr,* 1934, **68**, 2.

[25] **Kuhn, W.**, *Kolloidschr*, 1936, **76**, 258.

[26] **Guth, E. and Mark, H.**, *Monotsch. Chem.,* 1934, **64**, 93.

[27] **Durmaz S, Okay O.** *Polymer Bulletin* 2001**; 46**; 409

[28] **Durmaz S, Okay O.** *Polymer* 2002; **43**; 1215

[29] **Sedlakova, Z., Bouchal, K., Ilavsky, M.**, *Polym. Gels. Networks*., 1998, **6**, 63.

[30] **R.E. Hummel,** Understanding Materials Science, Springer, New York, 1998.

[31] **B. Velde,** Introduction to Clay Minerals, Chapman and Hall, London, 1992.

[32] **Fossum J. O**. *Physica A*, 1999, **270**, 270

[33] **Tjong S.C.** , *Materials Science and Engineering R,* 2006, **53,** 73–197

[34] Laponite Product Datasheet, Rockwood Chemicals, UK

[35] **P.K. Jennes**, Laporte Technical Reports, Laporte Absorbents, UK.

[36] **Alexandre, M.**; **Dubois, P**. *Mater. Sci. Eng.* 2000, ***28***, 1.

[37] **Chen B. Evans J.R.G.** *J. Phys. Chem. B* 2004, ***108,*** 14986

[38] **Vaia RA, Price G, Ruth PN, Nguyen HT, Lichtenhan J.**, *Appl Clay Sci,* 1999;**15**:67

[39] **Giannelis EP.** *Appl Organomet Chem,* 1998;**12** :675

[40] **Xu R, Manias E, Snyder AJ, Runt J.** *Macromolecules* 2001;**34**:337

[41] **Gilman JW**. *Appl Clay Sci,* 1999;**15**:31

[42] **Sinha Ray S, Yamada K, Okamoto M, Ueda K.** *Nano Lett* 2002;**2**:1093

[43] **A. Okada, M. Kawasumi, T. Kurauchi, O. Kamigaito**, *ACS Polym. Prepr*. 1987, **28**, 447

[44] **Pinnavaia, T. J.** *Science* 1983**, 220**, 365.

[45] **Carrado, K. A.** *Appl. Clay Sci.* 2000, **17**, 1.

[46] **Powell C.E., Beall G.W.**, *Current Opinion in Solid State and Materials Science*, 2006, **10** 73

[47] **Haraguchi K., Li H.J.**, *Macromolecules* 2006, **39**, 1898

[48] **Okay O, Balimtas NK, *and* Naghash HJ**, *Polymer Bulletin,* 1997, **39**, 233-239

[49] **Keskinel M, and Okay O**, *Polymer Bulletin*, 1998, **40**, 491

[50] **Durmaz S, Okay O**. *Polymer* 2000;**41**:3693

[51] **Baghdadi HA, Sardinha H, Bhatia SR. J** *Polym Sci B Polym Phys* 2005;**43**:233

[52] **Pozzo DC, Walker LM.** *Colloids Surf A* 2004;**240**:187

[53] **J. Zebrowski, V. Prasad, W. Zhang, L. M. Walker and D. A. Weitz,** *Colloids and Surfaces A: Physicochem. Eng. Aspects*, 2003, **213,** 189

[54] **Can V, and Okay O,** *Designed Monomers Polymers*, 2005, **8**, *453*

[55] **Ilavsky M., Hrouz J. Stejskal J., Bouchal K.**, 1984, *Macromolecules* **17**, 2868

AUTOBIOGRAPHY

Volkan Can was born in Istanbul in 1981. He has graduated from Beşiktaş Atatürk Anatolian High School in 1999 and after that he has graduated from the Chemistry Program – ITU in 2005. He has started the Polymer Science and Technology program right after the graduation and worked with Prof. Dr. Oğuz OKAY in his MSc. research.